CONFIDENTIAL
"This material contains information affecting the National Defense of the United States within the meaning of the Espionage Laws, Title 18, U. S. C. Sec. 793 and 794, the transmission or revelation of which in any manner to an unauthorized person is prohibited by law."

X70-17992

Classification changed to Unclassified per authority of NASA Hqs Memo 12/11/71

NASA CR66991

ufn 2/5/75

[redacted]

OCT 1975 RECEIVED NASA STI FACILITY INPUT BRANCH

DOWNGRADED AT 3 YEAR INTERVALS; DECLASSIFIED AFTER 12 YEARS DOD DIR 5200.10

AUG 1975 RECEIVED NASA STI FACILITY INPUT BRANCH

CONFIDENTIAL

CLASSIFIED BY HA Hedquist LaRC Chief Officer SUBJECT TO GENERAL DECLASSIFICATION SCHEDULE OF EXECUTIVE ORDER 11652 AUTOMATICALLY DOWNGRADED AT TWO YEAR INTERVALS AND DECLASSIFIED ON DEC 31 1976

GARRETT

AIRESEARCH MANUFACTURING COMPANY
A DIVISION OF THE GARRETT CORPORATION
9851-9951 SEPULVEDA BLVD. • LOS ANGELES, CALIFORNIA 90009
TELEPHONE: SPRING 6-1010, ORCHARD 0-0131 • CABLE: GARRETTAIR LOS ANGELES

(NASA-CR-66991) HYPERSONIC RESEARCH ENGINE PROJECT. PHASE 2A: AEROTHERMODYNAMIC INTEGRATION MODEL DEVELOPMENT, DATA ITEM NO. 55-4.05 Interim Technical Data Report no. 5, 10 Mar. - 9 Jun. 1969 (AiResearch Mfg. 00/98

N76-70994

Unclas 42375

CONFIDENTIAL
"This material contains information affecting the National Defense of the United States within the meaning of the Espionage Laws, Title 18, U. S. C. Sec. 793 and 794, the transmission or revelation of which in any manner to an unauthorized person is prohibited by law."

FORM 85877-D

~~CONFIDENTIAL~~
THIS PAGE IS UNCLASSIFIED

CR66991

THE GARRETT CORPORATION
AiResearch Manufacturing Division
LOS ANGELES 45, CALIFORNIA

Classification changed to Unclassified per authority of NASA Hqs Memo 12/11/74 ufn 2/5/75

REPORT NO. AP-69-5298

HYPERSONIC RESEARCH ENGINE PROJECT - PHASE IIA AEROTHERMODYNAMIC INTEGRATION MODEL DEVELOPMENT FIFTH INTERIM TECHNICAL DATA REPORT (U) DATA ITEM NO. 55-4.05 10 MARCH THROUGH 9 JUNE 1969 NASA CONTRACT NO. NAS1-6666

AP-69-5298 8 July 1969

CLASSIFIED DOCUMENT - UNCLASSIFIED TITLE

This material contains information affecting the national defense of the United States within the meaning of the espionage laws, Title 18, U.S.C., Sections 793 and 794, the transmission or revelation of which in any manner to an unauthorized person is prohibited by law.

Group 4

Downgraded at 3 year intervals; declassified after 12 years DOD DIR 5200.10

NO. OF PAGES 51

PREPARED BY Engineering Staff

DATE 8 July 1969

EDITED BY L. F. Jilly

Attachment: AiResearch Drawings
L-950991
L-950981
PA-106753
950512

APPROVED BY Henry J. Lopez
Henry J. Lopez
HRE Program Manager

REVISIONS				ADDITIONS			
PAGE	DATE	PAGE	DATE	PAGE	DATE	PAGE	DATE

~~CONFIDENTIAL~~
THIS PAGE IS UNCLASSIFIED

FOREWORD

This interim technical data report is submitted to the NASA Langley Research Center by the AiResearch Manufacturing Company, Los Angeles, California. The document was prepared in accordance with the guidelines established in paragraph 6.3.3.2 of NASA Statement of Work L-4947-B.

Interim technical data reports are generated on a quarterly basis for major program tasks under the Hypersonic Research Engine (HRE) Project. Upon completion of a given task effort a final technical data report will be submitted.

This document presents a detailed technical discussion of the development of the Aerothermodynamic Integration Model (AIM) and covers the period of 10 March through 9 June 1969.

ACKNOWLEDGEMENTS

Acknowledgements for contributions to this document are hereby extended to the following persons:

L. Kado K. Mastin	Technical Coordination
Dr. Sun L. Pearson W. Sainio	Aerodynamics
F. Walters S. Cho	Heat Transfer Analysis
W. Flieder J. Hancock	Stress Analysis
J. Davis A. Heller W. Gallagher	Design

CONTENTS

Section		Page
1.	SUMMARY OF STATUS	1-1
	1.1 Overall Model Design	1-1
	1.2 Hardware	1-1
	1.3 Tests	1-1
2.	PROBLEM STATEMENT	2-1
3.	TOPICAL BACKGROUND	3-1
4.	OVERALL APPROACH	4-1
5.	ANALYTICAL DESIGN	5-1
	5.1 Aerodynamic Analysis	5-1
	5.2 Structural Design Analysis	5-7
	5.3 Heat Transfer Analysis	5-12
6.	DESIGN AND FABRICATION	6-1
	6.1 Subassembly Status	6-1
7.	FUTURE ACTION	7-1
	7.1 Design Activity	7-1
	7.2 Tests	7-1
	REFERENCES	R-1
Appendix		
A	INLET-COMBUSTOR INTERACTION MODEL ANALYSIS	A-1
B	CONVERSION OF IDEAL GAS TEST RESULTS	B-1

ILLUSTRATIONS

Figure		Page
3.0-1	Aerothermodynamic Integration Model Nomenclature	3-2
5-1	Inlet Unstart Throat Mach Number and Pressure Rise	5-2
5-2	Peak Combustor Pressure Rise	5-4
5-3	Inlet Unstart Fuel Flow Limit	5-5
5-4	Nodal System for Nickel Tip of Outerbody Leading Edge (0.1 in. tip)	5-14
5-5	Nodal System for Nickel Tip of Outerbody Leading Edge (0.125 in. tip)	5-15
5-6	Nodal System for Nickel Tip of Outerbody Leading Edge (0.15 in. tip)	5-16
5-7	Tip Section of Outerbody Leading Edge - Nickel Walls	5-20
5-8	Cooling of Outerbody Leading Edge Tip - Zirconium-Copper Tip	5-21
6-1	Igniter Assembly, Disassembled	6-3
6-2	Igniter Assembly, Rear View	6-4
6-3	Igniter Assembly, Front View	6-5
A-1	Pitot Pressure Profiles, M_o = 6.05	A-3
A-2	Pitot Pressure Profiles, M_o = 8.0	A-4

TABLES

Table		Page
5-1	Steady State Temperature Distribution in Nickel Tip of Outerbody Leading Edge Shown in Figure 5-4	5-17
5-2	Steady State Temperature Distribution in Nickel Tip of Outerbody Leading Edge Shown in Figure 5-5	5-18
5-3	Steady State Temperature Distribution in Nickel Tip of Outerbody Leading Edge Shown in Figure 5-6	5-19

1. SUMMARY OF STATUS

1.1 OVERALL MODEL DESIGN

The analytical effort for this period was devoted to completing the heat transfer analysis and stress analysis of the outer shell. Effort also was expended in reanalyzing the design change incorporating a zirconium-copper tip on the cowl leading edge and the inlet spike.

The inlet spike was also modified to incorporate another fuel injector manifold 4.25 in. downstream from fuel injector 1A. The second injector on the spike assembly has been designated injector 1C.

Detail drawing of the outer cowl will be completed by 7 July 1969.

1.2 HARDWARE

Fabrication of the detail hardware for the nozzle plug and the nozzle shroud is progressing satisfactorily, with completion of the assembly scheduled for August of 1969. Sections of the inlet spike assembly not affected by the design change are progressing satisfactorily, and are now in the subweldment stage.

1.3 TESTS

Initial tests on the igniter assembly have been completed, and basic design and exciter requirements established. Further testing of the igniter to determine endurance life and range of operation will be made during the next reporting period.

2. PROBLEM STATEMENT

The objective of the Aerothermodynamic Integration Model (AIM) is to verify the feasibility of integrating various analytical and experimental data obtained for the design of the Hypersonic Ramjet Engine, and to evaluate the overall engine performance of this design. The design of this model will be directed to evaluating aerodynamic characteristics without major concern for the structural life of the model.

3. TOPICAL BACKGROUND

The Aerothermodynamic Integration Model (AIM) will be a water-cooled, ground-test model of the Hypersonic Research Engine.

The nomenclature used to describe the various aerodynamic surfaces of this engine is shown in Figure 3.0-1.

General design guides to be followed in the design of the AIM will be (1) the aerodynamic contours of the AIM will be those obtained from component testing wherever possible, (2) the surface temperature of the engine will be dictated by the maximum metal temperature allowable for structural integrity and by requirements of preventing boiling of the water used as the coolant, and (3) in order that the engine may be tested over the range from Mach 3 to 8, the inlet spike will be mechanized to permit translation.

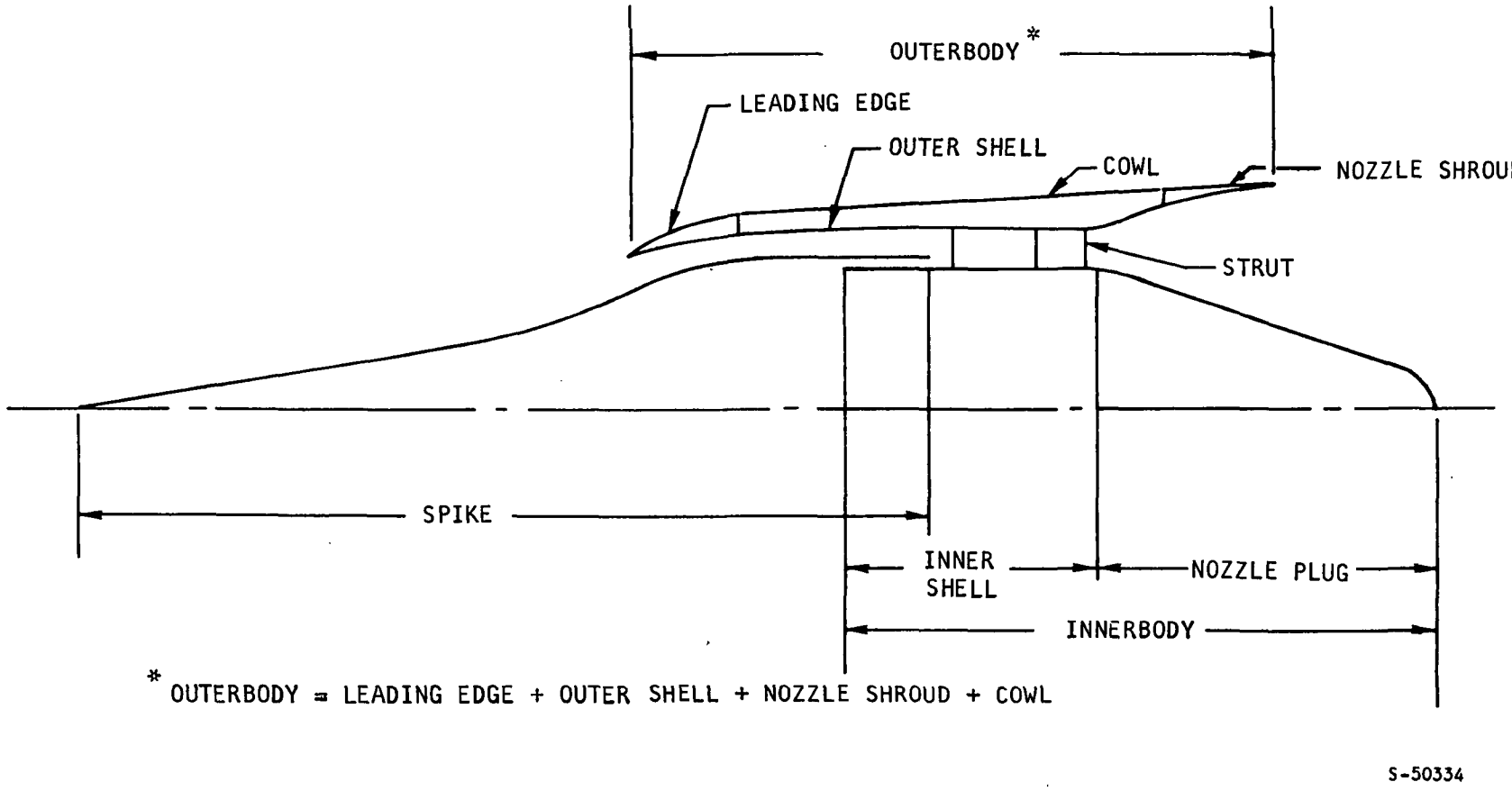

Figure 3.0-1. Aerothermodynamic Integration Model Nomenclature

4. OVERALL APPROACH

The basic design concepts previously submitted were used in the component layout drawing. However, due to the diverse requirements imposed upon the design to satisfy the considerations of thermal analysis, structural design, mechanical design and manufacturing techniques, tests will be conducted to determine the internal aerodynamic performance over Mach number range of 4.0 to 7.0. The effects of varying inlet air total pressure and temperature, fuel-air ratio, inlet spike position, and combustion mode will be investigated. All tests will be conducted with clean air. The measured performance will have to be corrected to account for heat removed by the water-cooling system.

Tests will be performed in two series. The first will be oriented toward (1) evaluating the inlet-combustor interaction and stability, (2) evaluating the performance of the positive ignition system, (3) identifying conditions when autoignition is feasible, (4) demonstrating combustion mode transition, and (5) evaluating inlet and combustor performance.

The second series of tests will be performed to (1) determine overall engine performance, (2) determine engine operating characteristics with feasible variations in fuel equivalence ratio, and (3) determine nozzle performance for the purpose of substantiating the predicted overall engine performance, including chemical kinetic effects.

Group 4

Downgraded at 3 year intervals;
declassified after 12 years
DOD DIR 5200.10

This material contains information affecting the national defense of the United States within the meaning of the espionage laws, Title 18, U.S.C., Sections 793 and 794, the transmission or revelation of which in any manner to an unauthorized person is prohibited by law.

5. ANALYTICAL DESIGN

5.1 AERODYNAMIC ANALYSIS

5.1.1 Inlet-Combustor Interaction

Analysis of the experimental data from the two-dimensional combustor test rig and the 2/3-scale inlet model test indicates that there is need to consider provisions for injecting fuel further downstream than that presently planned. Ideally, one would like to add all of the fuel from the first stage for supersonic combustion from Mach 6 to 8; however, as fuel flow is increased, the flow separation due to shock-boundary layer interaction upstream of the fuel injector is also increased. Severe flow separation could cause the engine inlet to unstart. In order to assess this problem and to determine the maximum amount of fuel that can be injected into the first stage, and also its consequences on engine performance, the following analyses were made:

5.1.1.1 Inlet Unstart Criteria

To establish the inlet unstart criteria a flow model is postulated as shown below:

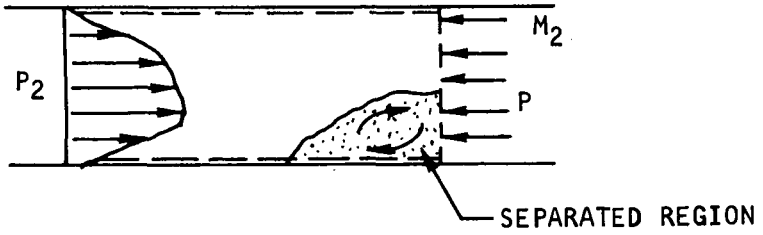

It is assumed that the inlet will unstart if the flow Mach number reaches certain minimum values. From momentum considerations, if it is assumed that the momentum ($\dot{m}v$) associated with separated flow is negligible and only the pressure force is considered, maximum pressure rise can then be calculated for each assumed Mach number from the conservation equations. The results are shown in Figure 5-1. The detailed calculation and procedures are given in Appendix A.

From the 2/3-scale inlet model test with helium injection at the throat, it was indicated that the inlet would unstart at a pressure ratio (P/P_2) of 3 at Mach 8, and 2.3 at Mach 6, where P_2 is the undisturbed throat static pressure. Superimposing the unstart test data (pressure rise) on Figure 5-1, the Mach numbers which would unstart the inlet are 1.7 for Mach 6 and 2.42 for Mach 8.

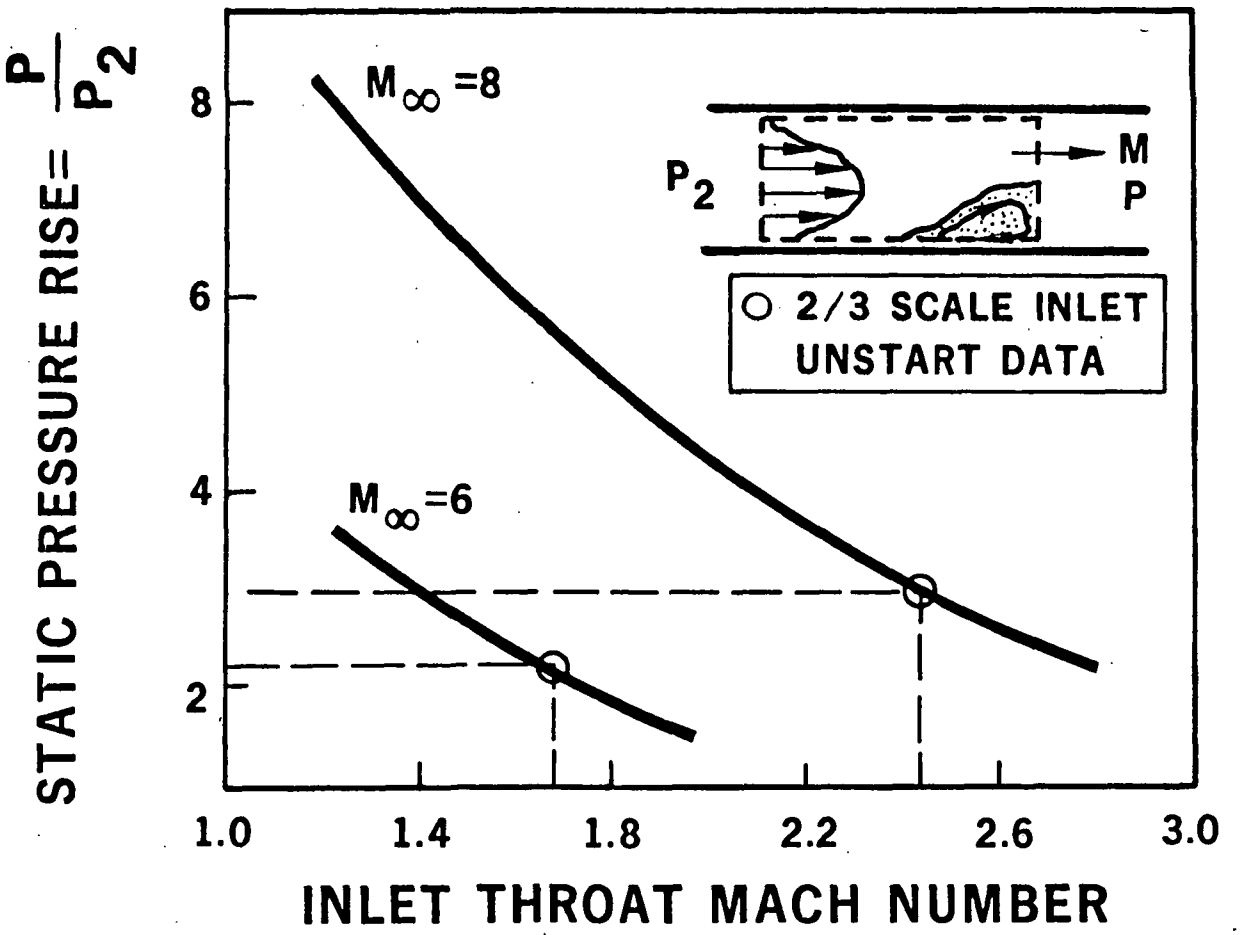

Figure 5-1. Inlet Unstart Throat Mach Number and Pressure Rise (U)

(U) It must be noted that the inlet unstart data was at low inlet total temperatures and for contraction ratios slightly different than the AIM inlet. Therefore, the unstart pressure ratios for the real-gas case were calculated assuming that the inlet unstarts at the same throat-Mach number as the ideal gas and that the mass-momentum averaged-total-pressure recovery (Reference 5-1) for both cases are the same. The procedure used to obtain these maximum pressure rises for the real gas is given in Appendix B; at Mach 6 the pressure rise increased to 2.64; at Mach 8 to 3.97.

5.1.1.2 Fuel Injection

(U) After the allowable combustor pressure rise had been determined, the next step is to correlate pressure rise with equivalence ratio. In Figure 5-2, the peak-pressure ratios for three different inlet total temperatures equivalent to Mach 5, 6, and 7 are plotted. It indicates that for the same equivalence ratio, the peak-pressure ratio is significantly reduced as the flight Mach number is increased. This is due to the combination effects of increasing temperature and specific heats. For Mach 8, it is estimated that at a ϕ of one, the peak-pressure ratio will be about 4 to 4.5.

(U) Using the above test data and the calculated unstart pressure rises, Figure 5-3 was derived. In addition to the first stage fuel flow limits, the static pressure rise P/P_∞ for different Mach numbers is also shown for reference. The amount of fuel that can be injected at the inlet throat station is shown on the bottom curve (on the right) and the top curve indicates the amount of fuel that can be injected into the first stage if the opposite injectors in the first stage are spaced 4 in. apart. This is based on the assumption that the local flow separation from the first injector will be reattached in 4 in.

5.1.2 Engine Performance

(C) In order to predict AIM engine performance, inlet, combustor, and nozzle test results were used. The calculated mass-momentum averaged-pressure recoveries (Appendix A) were used to obtain inlet performance. Combustor chemical efficiency plots versus length, and combustor pressure rise versus heat release for different area ratios were used to obtain combustor performance (combustor test data shall be presented in the next combustor TDR).

(C) For Mach 8 engine performance, extrapolation from combustor test results indicates an equivalence ratio of one with 97-percent chemical efficiency (η_c) could be obtained in a combustor length of 12.5 in., resulting in a combustor area ratio of 2.9. The estimated combustor exit pressure (P_4) for this chemical efficiency and area ratio is 0.77 P_2, where P_2 is the inlet throat undisturbed pressure. Using a combustor friction coefficient of 0.005, the following engine performance was obtained from I_{vac} charts (continuity-momentum chart):

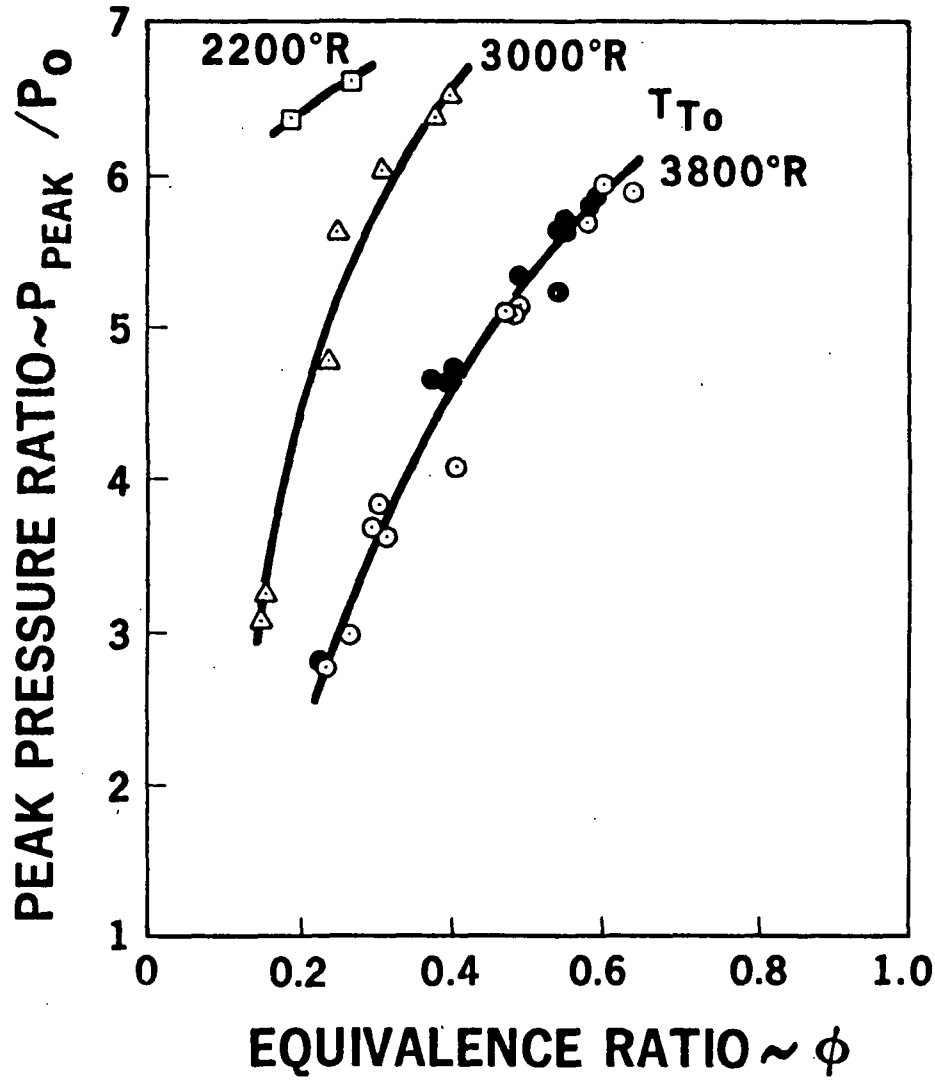

Figure 5-2. Peak Combustor Pressure Rise (U)

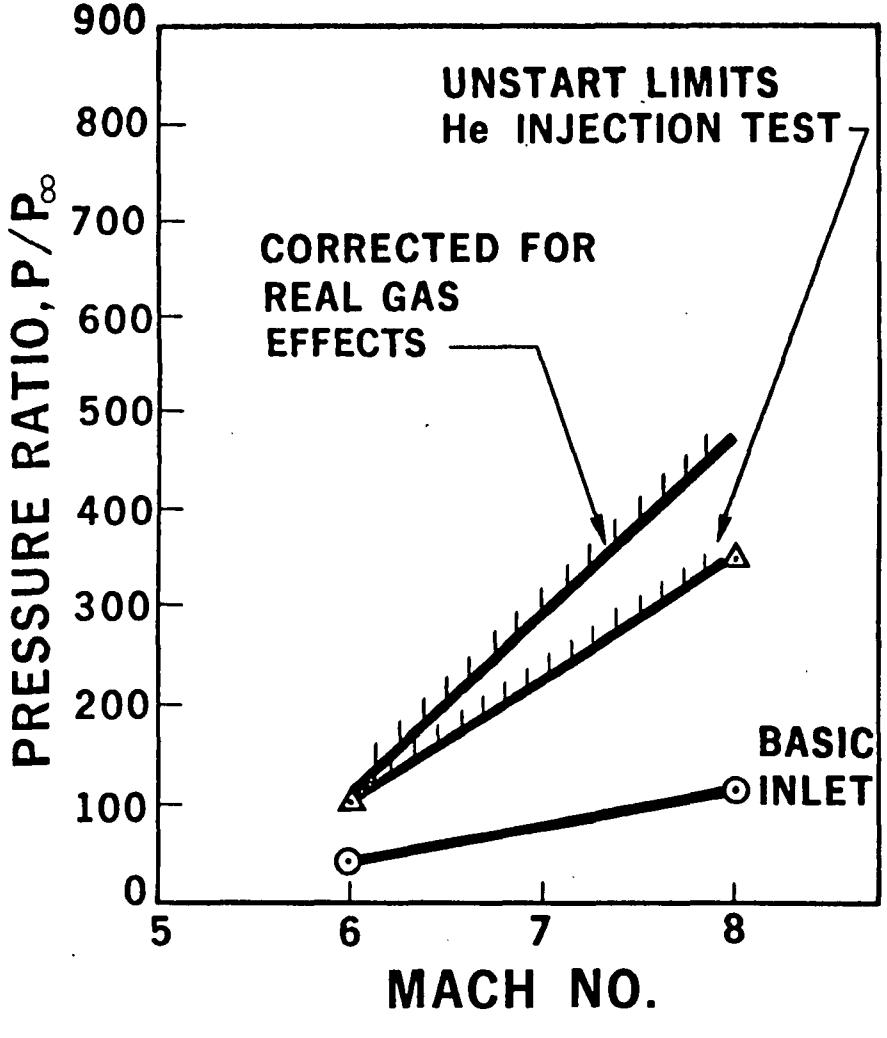

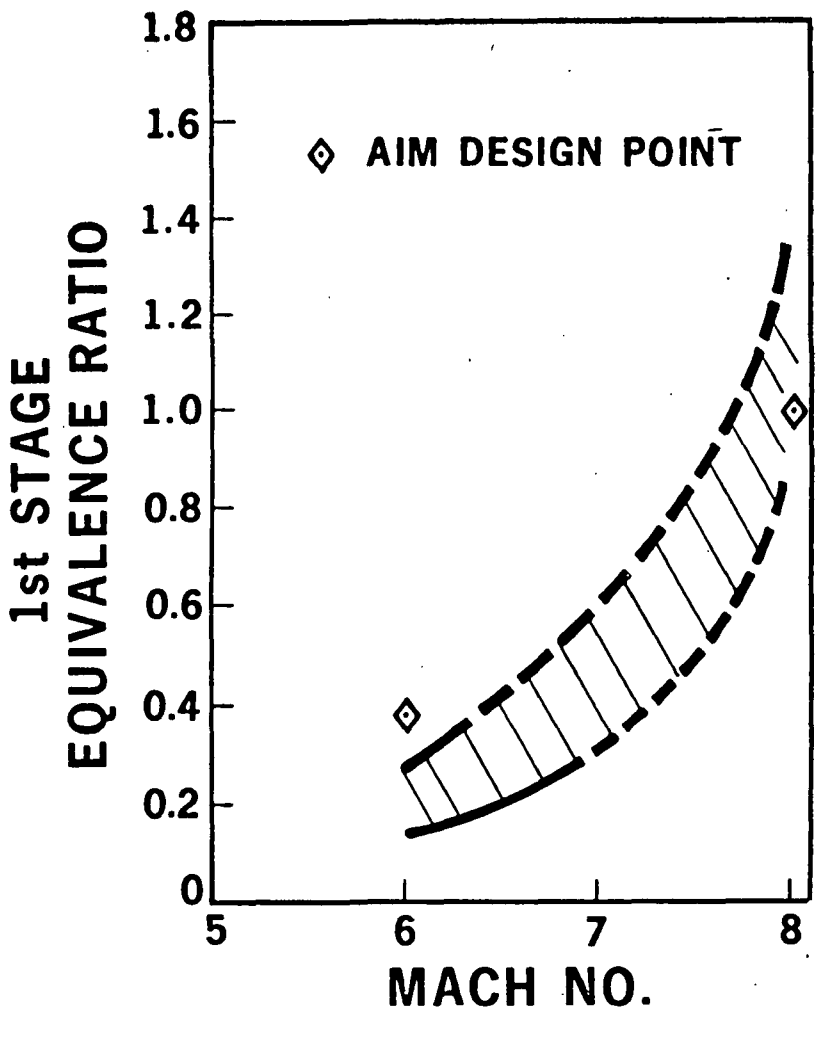

Figure 5-3. Inlet Unstart Fuel Flow Limit (U)

(C)

	$I_{vac}(\phi = 1, \eta_c = 0.97)$	Area, $in.^2$	A_4/A_2
Inlet Throat Sta. 40.5	225	17.92	1
Combustor Exit Sta. 53	289.8	52	2.9
Thermal Throat Sta. 64	279.4	90	---
Nozzle Exit	317.8	508.9	---

(U) For a nozzle efficiency (C_s) of 0.9658, fuel specific impulse of 2360 sec and thrust coefficient of 0.564 were obtained.

(U) For Mach 6 engine performance, Figure 5-3 shows that an equivalence ratio of 0.2 may be injected into the first stage. From the two-dimensional combustor test results, a chemical efficiency of 80 percent can be achieved in 8 in., which corresponds to an area ratio of 1.31 in the AIM engine. For this area ratio and combustor efficiency, the correlated pressure rise ratio was 1.47. Knowing the chemical efficiency and pressure-rise ratio, the combustor performance for the first stage is uniquely determined ($C_f = 0.005$).

(C) The remaining fuel of $\phi = 0.8$ is injected in the second stage. An overall chemical efficiency of 97 percent can be achieved in an additional 14 in. The extrapolated data showed that there would be no static pressure rise at the second stage exit. Using I_{vac} charts, (nozzle $C_s = 0.968$) a fuel specific impulse of 2690 sec and a thrust coefficient of 0.863 were obtained. The I_{vac} at combustor inlet, first and second combustor exists, and nozzle exit are shown in the following table.

(C)

	I_{vac}	Area, $in.^2$	A_4/A_2
Inlet Throat Sta. 40.5	157.9	30.48	1
First Stage Combustor Exit Sta. 48.5 ($\phi = 0.2$, $\eta_c = 0.80$)	160.7	39.8	1.31
Second Stage Combustor Exit Sta. 61.9 ($\phi = 1$, $\eta_c = 0.97$)	199.6	90	2.95
Nozzle Exit	265.1	508.9	---

It should be noted that the supersonic combustion performance at Mach 6 and Mach 8 have not been significantly altered from previous estimates (Reference 5-2).

5.2 STRUCTURAL DESIGN ANALYSIS

The following structural design analysis of the HRE AIM outer shell was performed during this reporting period.

5.2.1 Ground Rules

The following set of design ground rules was used in the outerbody analysis:

(a) The most severe aerodynamic conditions seen by the outer shell will be with freestream conditions of: $M_\infty = 7.00$, $P_{T_\infty} = 1200$ psia, and $T_{T_\infty} = 3820^0R$, combined with sustained combustion of the engine.

(b) The outer shell water-coolant flow circuit will be proof-tested to 1.5 x operating pressure.

(c) The outer shell will be capable of withstanding a 3-g-operating and a 5-g-transportation inertia load in any axis.

(d) Material factors of 1.5 on the ultimate material strength and 1.175 (85 percent of σ_{yield}) on the yield strength were used to establish allowable design stresses for operating conditions. In all cases, the yield criteria governed.

5.2.2 Analysis

The outer shell consists of a Hastelloy X cold shell, Hastelloy fins and a Nickel-200 hot shell. A third Hastelloy C shell was added to the forward section to provide means of properly distributing the coolant to the outer shell.

The two critical loads in the finned section are (1) the coolant pressure containment loads, and (2) the differential temperature thermal loads.

The critical case for the coolant pressure loads occurs when 330 psi is applied during proof-pressure test. (330 psi equals 1.5 x 220 psi, where 220 psi is the maximum coolant loop inlet pressure for the outerbody coolant circuit.) The fins used in the general outer shell area will have the following configuration: 16 fins per in., 0.154 in. high, manufactured from 0.006-in.-thick Hastelloy X material.

The stress to which the fins will be subjected during proof-pressure test can be calculated as follows.

$$\sigma = \frac{P \times k(1 - A_{fins})}{A_{fins}}$$

$$\sigma = \frac{330 \times 3(1 - 16 \times 0.006)}{16 \times 0.006} = 9300 \text{ psi}$$

where p = proof pressure

A = fin tensile area

k = fin stress concentration factor

The yield strength of the Hastelloy X is 45,000 psi for the environment considered.

The Hastelloy shell was designed to carry the internally reacted unsymmetric unstart load, the coolant pressure load, and the thermal load imposed by the nickel hot-skin.

The unsymmetric unstart load was considered to act as a point load of 11,400 lb applied at Sta 43.30. This load is reacted by the six struts connecting the outer and inner bodies at Sta 60.50. The bending introduced in the shell is equal to 11,400 lb x (60.50 - 43.30) = 196,000 in.-lb.

The section modulus of the shell at Sta 60.50 may be calculated as follows

$$Z = \pi R^2 t$$

$$= \pi(11.5)^2(0.200)$$

$$= 83.0 \text{ in.}^3$$

where R = radius, in.

t = thickness, in.

Stress in bending is

$$\sigma_{bending} = \frac{M}{Z} = \frac{196{,}000 \text{ in.-lb}}{83.0 \text{ in.}^3} = 2360 \text{ psi}$$

The stress level around the strut socket was considered and determined to be well below the yield strength of Hastelloy under the applied bending load.

The Hastelloy shell thickness was also sized to restrict hoop stress to remain within the elastic range due to the 330 psi coolant proof pressure. The hoop stress in the Hastelloy shell, if the restraint of the nickel were neglected is:

$$\sigma = \frac{pr}{t} = \frac{(330)(11.5)}{0.2} = 19{,}500 \text{ psi}$$

This stress is also well below the yield value for Hastelloy X at room temperature.

The tensile stress imposed on the Hastelloy shell by the thermal expansion of the nickel innerbody is exactly equal to the compressive stress in the nickel shell since they are the same thickness. Since the nickel shell yields in compression due to its lower yield strength, the maximum plastic stress in the nickel is also the tensile stress in the Hastelloy shell.

This plastic stress was calculated using a nickel shell skin temperature of $1000^{\circ}F$ and a Hastelloy shell temperature of $100^{\circ}F$. The plastic strain in the nickel shell equals the total deformation minus the equivalent elastic deformation of the nickel and Hastelloy shells:

$$\epsilon_{plastic} = \epsilon_{total} - \epsilon_{elastic}$$

$$\epsilon_{plastic} = \alpha\Delta T - 2\frac{\sigma_{yield\ NI}}{E_{elastic}} - 2\frac{\sigma_{Hast\ X}}{E_{Hast\ X}}$$

$$\sigma_{yield\ nickel} = 8600 \text{ psi (after three braze cycles)}$$

$$E_{elastic\ at\ temp} = 16 \times 10^{6} \text{ psi (nickel)}$$

$$\alpha\Delta T = (8.0 \times 10^{-6} \text{ in./in.-}^{\circ}F)(900^{\circ}F) = 0.0072 \text{ in./in.}$$

$$\epsilon_{plastic} = 0.0072 \text{ in./in.} - \frac{2 \times 8600 \text{ psi}}{16 \times 10^{6} \text{ psi}} - \frac{2 \times 8600 \text{ psi}}{26 \times 10^{6} \text{ psi}}$$

$$= (0.0072 - 0.001075 - 0.00066) \text{ in./in.}$$

$$\epsilon_{p} = 0.00606 \text{ in./in. plastic strain}$$

From the Nickel-200 stress/strain curve (after braze cycling), this corresponds to an operating compressive stress in the nickel of 9900 psi. This is also equal to the operating stress in the Hastelloy shell. Superimposing this thermal stress and the unsymmetric unstart bending stress gives a total stress of 12,000 psi which is well below the yield strength of the Hastelloy shell.

To calculate the thermal cyclic life of the nickel hot shell, the equivalent triaxial resultant strain was calculated using the Von Misses Distortion Energy Theorem:

$$\epsilon_{eq} = \frac{\sqrt{2}}{3}\left[(\epsilon_1 - \epsilon_2)^2 + (\epsilon_2 - \epsilon_3)^2 + (\epsilon_3 - \epsilon_1)^2\right]^{1/2}$$

$\epsilon_1 = \epsilon_2 = 0.00606$ in./in. (equal biaxial surface strains)

From the constant volume relationship

$$\epsilon_1 + \epsilon_2 + \epsilon_3 = 0 \quad \text{or} \quad \epsilon_3 = -2\epsilon_1 = -2\epsilon_2$$

Substituting $\epsilon_2 = \epsilon_1$ and $\epsilon_3 = -2\epsilon_1$ into triaxial strain formula:

$$\epsilon_{eq} = \frac{\sqrt{2}}{3}\left[(\epsilon_1 - \epsilon_1)^2 + (\epsilon_1 + 2\epsilon_1)^2 + (-2\epsilon_1 - \epsilon_1)^2\right]^{1/2}$$

or $$\frac{\sqrt{2}}{3}\left[2(3\epsilon_1)^2\right]^{1/2} = 2\epsilon_1$$

$$\epsilon_{eq} = 2(0.00606 \text{ in./in.}) = 0.01212 \text{ in./in.}$$

$$N = \text{cycles to failure} = \left(\frac{C}{\epsilon_{eq}}\right)^2$$

where C = ductility constant of 0.3

$$N = \left(\frac{0.3}{0.01212}\right)^2 = (24.7)^2 = 610 \text{ cycles}$$ (at the most severe operating conditions)

Since the severe thermal gradients are only imposed during the high Mach number test conditions, this cyclic life is acceptable.

The outerbody also performs the function of transmitting the externally applied aerodynamic loads to the mount legs through the fore and aft support rings. The most severe external load is the 17,460 lb axial design load. The effect of this load at the support ring/mount leg interface was analyzed using the MIT SABOR III axisymmetric shell program. The stress resultants obtained from this analysis were negligible and the resulting ring and shell stresses are below 10,000 psi. The shell and rings are Hastelloy X with a room temperature yield stress of 45,000 psi.

There are several sections within the outer shell which are not fully supported by fins. The maximum unsupported span length is 0.75 in. Buckling of the nickel hot shell was investigated using a modified Euler-column analysis. This nickel shell strain equals: $\epsilon = \alpha\Delta T$ where ΔT equals 900^0F. This provides a strain of: $(8.0 \times 10^{-6}$ in./in.-^{0}F) x 900^0F = 0.0072 in./in. (this strain indicates the skin is in the plastic range).

The equivalent stress for this strain is 10,500 psi. The tangent modulus for this strain value equals 0.84×10^6 psi. Using the basic Euler column formula and applying the tangent modulus instead of the elastic modulus, a relationship between the span length-to-thickness ratio and the critical stress can be developed.

Euler's equation

$$P_{cr} = \eta \frac{\pi^2 EI}{l^2}$$

for plastic end conditions,

$$\eta = 1$$

Substituting for the inertia of the shell and adding a Poisson's factor for two-dimensional effects, the equation becomes:

$$P_{cr} = \frac{\pi^2 E t^3}{12(1 - \nu^2)\, l^2}$$

Dividing by (t) to solve for critical stress:

$$\sigma_{critical} = \frac{P}{t} = \frac{\pi^2 E t^2}{12(1 - \nu^2)\, l^2}$$

assuming a Poisson's ratio of 0.4 and evaluating the constants

$$\sigma_{critical} = \frac{\pi^2 (0.84 \times 10^6)\, t^2}{12(0.84)\, l^2} = 825{,}000 \frac{t^2}{l^2}$$

or

$$\frac{l^2}{t^2} = \frac{825{,}000}{\sigma_{critical}}$$

Solving for the $\frac{l}{t}$ ratio for $\sigma_{critical}$ = 10,500 psi

$$\frac{l}{t} = \sqrt{\frac{825{,}000}{10{,}500}} = \sqrt{78.5} = 8.86$$

For t = 0.2 in., the allowable unsupported length is 1.772 in.

The hydrogen injector manifolds and injector tubes were analyzed for thermal fatigue and pressure containment. The manifolds were designed so that the hoop stress developed by the hydrogen internal pressure would remain within the elastic range of the material. This means the thermal yielding of the manifolds is the only plastic deformation and was the governing case for the cyclic design:

$$\epsilon_{plastic} = \epsilon_{total} - \epsilon_{elastic}$$

$$\epsilon_{plastic} = \alpha\Delta T - \frac{2\,\sigma_{yield}}{E_{elastic}}$$

$$= (8.0 \times 10^{-6}\ \text{in./in.})(1000^{\circ}\text{F}) - 2 \times \frac{41{,}500\ \text{psi}}{24.3 \times 10^{6}\ \text{psi}}$$

$$= 0.008\ \text{in./in.} - 0.0034\ \text{in./in.}$$

$$\epsilon_{plastic} = 0.0046\ \text{in./in.}$$

The cycle life may be calculated as follows using C = 0.3 (ductility constant)

$$N = \left(\frac{C}{\epsilon_p}\right)^2 = \left(\frac{0.3}{0.0046}\right)^2 = 4250 \text{ cycles to failure for manifolds}$$

The injector tubes will carry a tensile load during proof testing. Since they are located in a gap area with no fins, it was assumed that they carry the proof-pressure separating load over 0.5 in.^2.

$$\sigma_{tensile} = \frac{P(0.5)}{A_{tube}} = \frac{(330\ \text{lb/in.}^2)(0.5\ \text{in.}^2)}{(\pi)(0.15\ \text{in.})(0.03\ \text{in.})} = 11{,}700\ \text{psi}$$

This is also well below the tensile strength of Hastelloy X during the room temperature proof test.

5.3 HEAT TRANSFER ANALYSIS

During this reporting period, the heat transfer analytical effort was directed towards finalizing the outerbody cooling system, and in redesign of the cowl leading edge and the inlet spike. The redesign was initiated since the temperature increase reported in the 4th AIM TDR for the cowl leading edge and inlet spike which indicated the structural integrity of these items was in jeopardy.

Zirconium-copper was selected as the best candidate material among the copper alloys because of its superior structural properties, with coefficient

of thermal conductivity nearly equal to that of OFHC copper. Nickel was also considered as an alternate material and designs incorporating these materials are reported in this section.

5.3.1 Outerbody Cooling System

Completion of the outer shell design (Layout Drawing L-950991, attached at end of this report) finalizes the cooling system of the outerbody section which consists of the leading edge, outer shell and nozzle shroud. Heat transfer analysis on each section has been reported in References 5-3 and 5-4. The pressure drop for the redesigned cowl leading edge is approximately 10 psi greater than design previously reported, hence, the overall pressure drop for the outerbody section is calculated to be 195 psi.

The cowl leading edge was redesigned for reasons mentioned above. The candidate materials considered for the redesign were chromium-copper, zirconium-copper and nickel. The design incorporating zirconium-copper was selected, since this design best fulfilled requirements of design, fabrication, and low cost. A candidate design is described in detail below.

5.3.1.1 Nickel Cowl Leading Edge

Conduction lengths from the stagnation line to the coolant water of 0.1, 0.125, and 0.150 in. were considered as shown in Figures 5-4, 5-5, and 5-6. Steady state temperature distributions in these tip configurations are shown in Tables 5-1, 5-2, and 5-3. A coolant flow rate of 230 gpm, out of the total outerbody coolant flow rate of 660 gpm, was used for the analysis, with the remaining 430 gpm bypassing. The reduction in the coolant water flow rate in the tip section is necessary to maintain an acceptable coolant water pressure drop. From the results shown in Tables 5-2 to 5-3, the uncooled nickel tip length of 0.125 in. was selected, and from manufacturing and structural points of view, a flow configuration shown in Figure 5-7 was considered. Two sets of bypass holes were provided to keep the coolant pressure drop in the tip section at an acceptable level. The tip was to be cooled by 170-gpm water flowing through a 0.028-in.-U-bend gap. This coolant flow rate with the specified flow-gap gives about the same coolant velocity near the tip back surface as in the configuration of Figure 5-5. Therefore, the temperature distribution shown in Figure 5-5 and Table 5-2 is approximately valid for the nickel tip of Figure 5-7.

5.3.1.2 Zirconium-Copper-Tip Cowl Leading Edge

The zirconium-copper tip considered is shown in Drawing No. 950554 and Figure 5-8. Major changes from Reference 5-5 are (1) use of zirconium copper instead of OFHC copper for the tip, (2) reduction of the uncooled tip length from 0.6 in. to 0.3 in., (3) use of Hastelloy X fins for supporting the flow divider between the inner and outer coolant passages, and (4) bypass of the cooling water, as shown in Figure 5-8.

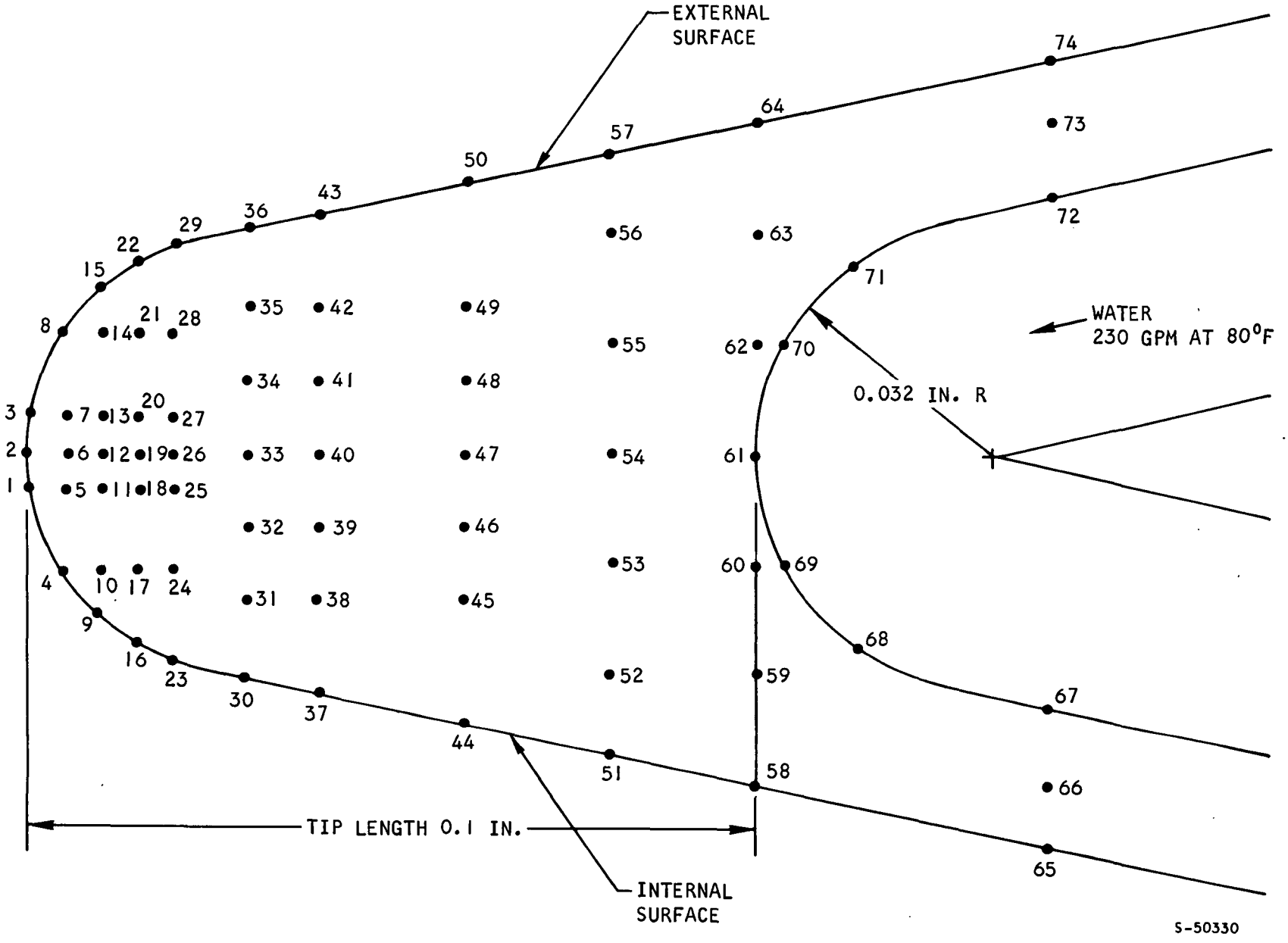

Figure 5-4. Nodal System for Nickel Tip of Outerbody Leading Edge (0.1 in. Tip)

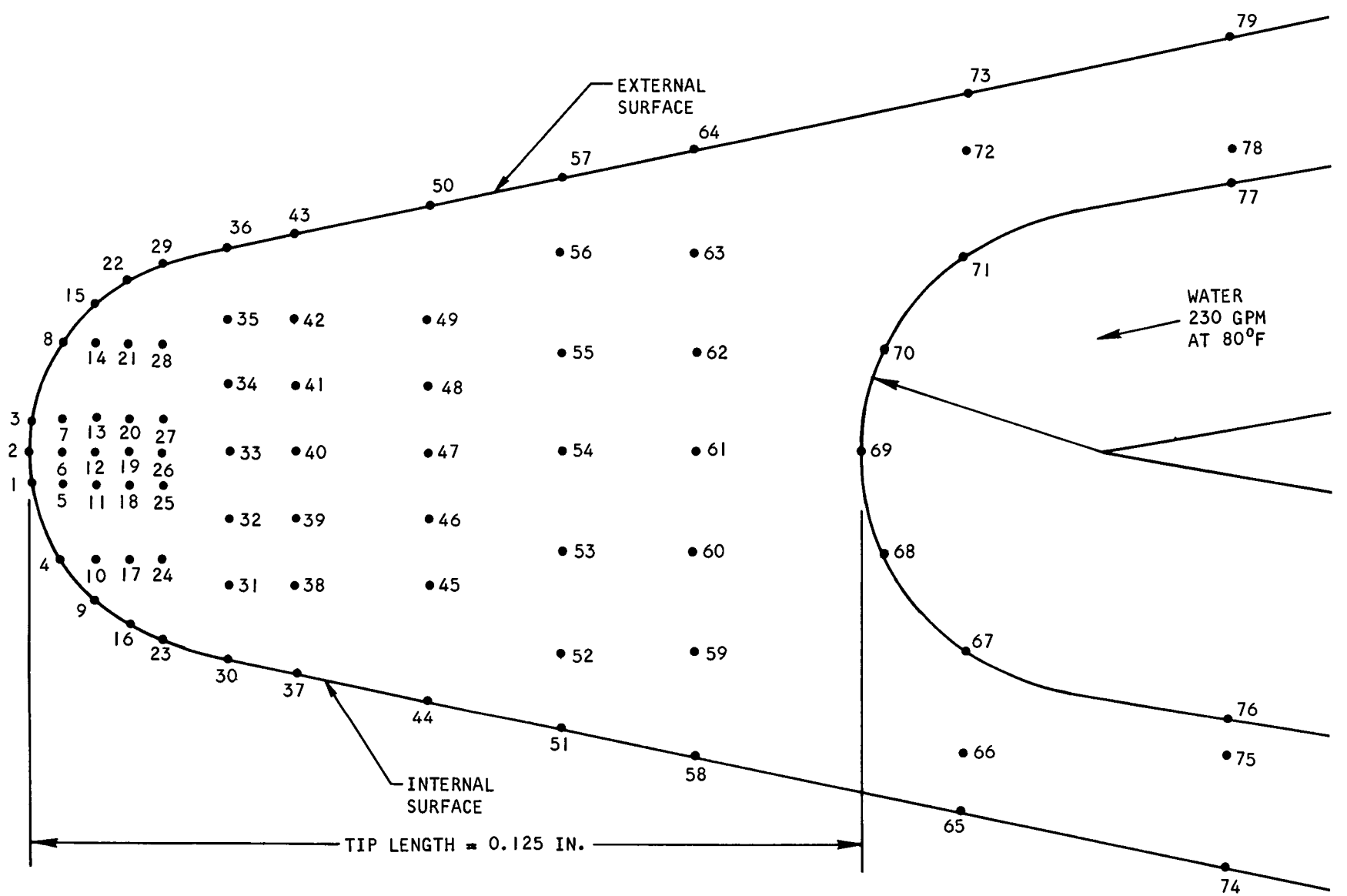

Figure 5-5. Nodal System for Nickel Tip of Outerbody Leading Edge (0.125 in. tip)

S-50335

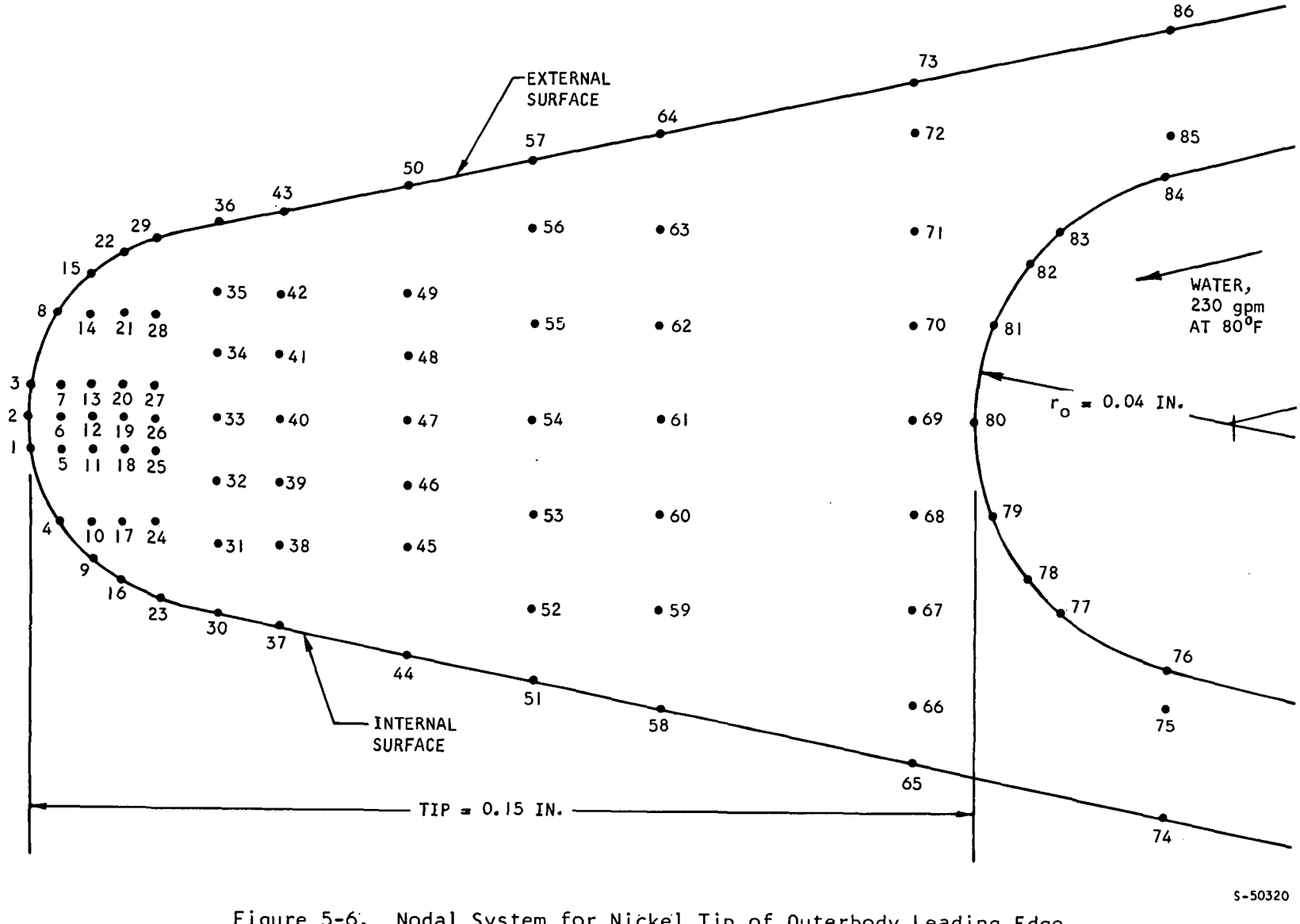

Figure 5-6. Nodal System for Nickel Tip of Outerbody Leading Edge (0.15 in. tip)

TABLE 5-I

STEADY STATE TEMPERATURE DISTRIBUTION IN NICKEL TIP OF OUTERBODY LEADING EDGE SHOWN IN FIGURE 5-4

Node	Temp, °F	Node	Temp, °F
T 1=	1367.43	T 38=	933.60
T 2=	1418.95	T 39=	937.47
T 3=	1342.74	T 40=	943.12
T 4=	1293.99	T 41=	950.96
T 5=	1312.95	T 42=	961.99
T 6=	1317.37	T 43=	982.12
T 7=	1298.89	T 44=	714.96
T 8=	1269.64	T 45=	719.94
T 9=	1236.11	T 46=	724.48
T 10=	1242.93	T 47=	731.56
T 11=	1254.76	T 48=	741.55
T 12=	1253.96	T 49=	754.02
T 13=	1247.91	T 50=	779.63
T 14=	1232.01	T 51=	496.60
T 15=	1230.54	T 52=	502.26
T 16=	1183.82	T 53=	502.53
T 17=	1191.81	T 54=	508.38
T 18=	1199.65	T 55=	530.16
T 19=	1199.35	T 56=	563.22
T 20=	1197.50	T 57=	585.12
T 21=	1190.81	T 58=	323.10
T 22=	1192.35	T 59=	301.68
T 23=	1135.23	T 60=	268.89
T 24=	1140.95	T 61=	255.64
T 25=	1146.47	T 62=	288.47
T 26=	1147.31	T 63=	356.36
T 27=	1147.69	T 64=	416.00
T 28=	1147.36	T 65=	158.63
T 29=	1153.28	T 66=	149.84
T 30=	1036.55	T 67=	129.08
T 31=	1037.41	T 68=	193.33
T 32=	1041.31	T 69=	228.66
T 33=	1045.62	T 70=	241.12
T 34=	1050.91	T 71=	214.94
T 35=	1059.29	T 72=	169.00
T 36=	1075.42	T 73=	222.16
T 37=	931.19	T 74=	257.28

NOTES: (1) Gas conditions: $M_\infty = 6.65$, $p_{T_\infty} = 1200$ psia, $T_{T_\infty} = 3770^\circ R$

(2) Spike shock impingement effects:

$$\frac{h\ (peak)}{h\ (F\text{-}R)} = 15.5,\ h\ (peak) = 0.171 \times 15.5 = 2.65\ Btu/sec\ ft^2\ ^\circ F$$

$$\Delta X\ (peak\ heating\ width) = \frac{2r_o}{25} = 0.0024\ in.$$

h (F-R) = Fay-Riddell stagnation heat transfer coefficient with spike shock inside cowl lip

(3) Upstream air turbulence effects (Reference 5-5).
Gas heat transfer coefficients around stagnation point except peak heating zones described above were multiplied by factor of 1.8:

h_{STAG} = 0.171 x 1.8 = 0.308 Btu/sec ft^2 °F with spike shock inside cowl lip
= 0.278 x 1.8 = 0.50 Btu/sec ft^2 °F with spike shock outside cowl lip

(4) Multiplication factor due to curvature on coolant heat transfer coefficient = 1.55 (Reference 5-5).
Coolant heat transfer coefficient at coolant impinging point = 8.38 Btu/sec ft^2 °F.

TABLE 5-2

STEADY STATE TEMPERATURE DISTRIBUTION IN NICKEL TIP OF OUTERBODY LEADING EDGE SHOWN IN FIGURE 5-5

Node	Temp, °F	Node	Temp, °F
T 1=	1556.69	T 41=	1181.35
T 2=	1603.22	T 42=	1191.32
T 3=	1534.48	T 43=	1209.36
T 4=	1490.31	T 44=	964.23
T 5=	1507.51	T 45=	971.02
T 6=	1511.54	T 46=	976.55
T 7=	1494.91	T 47=	984.12
T 8=	1468.58	T 48=	993.42
T 9=	1437.67	T 49=	1004.36
T 10=	1444.19	T 50=	1026.40
T 11=	1454.68	T 51=	757.81
T 12=	1454.32	T 52=	767.12
T 13=	1448.60	T 53=	776.01
T 14=	1434.64	T 54=	787.31
T 15=	1433.34	T 55=	805.78
T 16=	1390.71	T 56=	829.49
T 17=	1398.03	T 57=	846.06
T 18=	1405.24	T 58=	575.21
T 19=	1405.03	T 59=	575.37
T 20=	1403.43	T 60=	576.35
T 21=	1397.47	T 61=	576.81
T 22=	1398.91	T 62=	599.85
T 23=	1346.77	T 63=	637.89
T 24=	1352.08	T 64=	674.02
T 25=	1357.24	T 65=	260.08
T 26=	1358.09	T 66=	255.00
T 27=	1358.50	T 67=	220.34
T 28=	1358.30	T 68=	240.48
T 29=	1363.69	T 69=	259.16
T 30=	1257.37	T 70=	256.46
T 31=	1258.40	T 71=	265.66
T 32=	1262.24	T 72=	346.64
T 33=	1266.38	T 73=	377.65
T 34=	1271.32	T 74=	195.34
T 35=	1279.95	T 75=	161.55
T 36=	1293.51	T 76=	150.73
T 37=	1161.68	T 77=	222.81
T 38=	1164.48	T 78=	247.52
T 39=	1168.51	T 79=	318.21
T 40=	1174.05		

NOTES: (1) Gas conditions: $M_\infty = 6.65$, $p_{T_\infty} = 1200$ psia, $T_{T_\infty} = 3770^\circ R$

(2) Spike shock impingement effects:

$$\frac{h\ (peak)}{h\ (F\text{-}R)} = 15.5,\ h\ (peak) = 0.171 \times 15.5 = 2.65\ Btu/sec\ ft^2\ ^\circ F$$

$$\Delta X\ (peak\ heating\ width) = \frac{2r_o}{25} = 0.0024\ in.$$

h (F-R) = Fay-Riddell stagnation heat transfer coefficient with spike shock inside cowl lip

(3) Upstream air turbulence effects (Reference 5-5).
Gas heat transfer coefficients around stagnation point except peak heating zones described above were multiplied by factor of 1.8:

h_{STAG} = 0.171 x 1.8 = 0.308 Btu/sec ft^2 °F with spike shock inside cowl lip
= 0.278 x 1.8 = 0.50 Btu/sec ft^2 °F with spike shock outside cowl lip

(4) Multiplication factor due to curvature on coolant heat transfer coefficient = 1.55 (Reference 5-5).
Coolant heat transfer coefficient at coolant impinging point = 6.80 Btu/sec ft^2 °F.

TABLE 5-3

STEADY STATE TEMPERATURE DISTRIBUTION IN NICKEL TIP OF OUTERBODY LEADING EDGE SHOWN IN FIGURE 5-6

Node	Temp, °F	Node	Temp, °F
T 1=	1711.24	T 44=	1169.31
T 2=	1753.68	T 45=	1176.60
T 3=	1691.01	T 46=	1182.31
T 4=	1650.66	T 47=	1189.76
T 5=	1666.39	T 48=	1198.38
T 6=	1670.09	T 49=	1208.23
T 7=	1654.94	T 50=	1227.87
T 8=	1630.96	T 51=	976.89
T 9=	1602.88	T 52=	987.12
T 10=	1608.59	T 53=	999.44
T 11=	1618.49	T 54=	1012.34
T 12=	1617.91	T 55=	1028.74
T 13=	1612.99	T 56=	1047.65
T 14=	1600.02	T 57=	1061.55
T 15=	1598.86	T 58=	799.48
T 16=	1595.75	T 59=	806.38
T 17=	1566.48	T 60=	815.13
T 18=	1573.13	T 61=	827.92
T 19=	1572.97	T 62=	846.53
T 20=	1571.54	T 63=	870.29
T 21=	1566.15	T 64=	897.39
T 22=	1567.48	T 65=	449.24
T 23=	1519.65	T 66=	449.85
T 24=	1524.57	T 67=	435.89
T 25=	1529.36	T 68=	425.70
T 26=	1530.17	T 69=	428.77
T 27=	1530.59	T 70=	455.46
T 28=	1530.44	T 71=	498.52
T 29=	1535.39	T 72=	550.61
T 30=	1437.97	T 73=	573.56
T 31=	1439.04	T 74=	264.40
T 32=	1442.67	T 75=	229.90
T 33=	1446.59	T 76=	200.20
T 34=	1451.17	T 77=	213.15
T 35=	1458.16	T 78=	258.28
T 36=	1471.44	T 79=	281.66
T 37=	1350.45	T 80=	296.54
T 38=	1353.29	T 81=	294.95
T 39=	1357.22	T 82=	284.22
T 40=	1362.48	T 83=	251.40
T 41=	1369.24	T 84=	254.52
T 42=	1378.35	T 85=	303.16
T 43=	1394.75	T 86=	387.67

NOTES: (1) Gas conditions: $M_\infty = 6.65$, $P_{T_\infty} = 1200$ psia, $T_{T_\infty} = 3770^\circ R$

(2) Spike shock impingement effects:

$$\frac{h\ (peak)}{h\ (F\text{-}R)} = 15.5,\ h\ (peak) = 0.171 \times 15.5 = 2.65\ Btu/sec\ ft^2\ ^\circ F$$

$$\Delta X\ (peak\ heating\ width) = \frac{2r_o}{25} = 0.0024\ in.$$

h (F-R) = Fay-Riddell stagnation heat transfer coefficient with spike shock inside cowl lip

(3) Upstream air turbulence effects (Reference 5-5).
Gas heat transfer coefficients around stagnation point except peak heating zones described above were multiplied by factor of 1.8:

h_{STAG} = 0.171 x 1.8 = 0.308 Btu/sec ft^2 °F with spike shock inside cowl lip
= 0.278 x 1.8 = 0.50 Btu/sec ft^2 °F with spike shock outside cowl lip

(4) Multiplication factor due to curvature on coolant heat transfer coefficient = 1.55 (Reference 5-5).
Coolant heat transfer coefficient at coolant impinging point = 6.10 Btu/sec ft^2 °F.

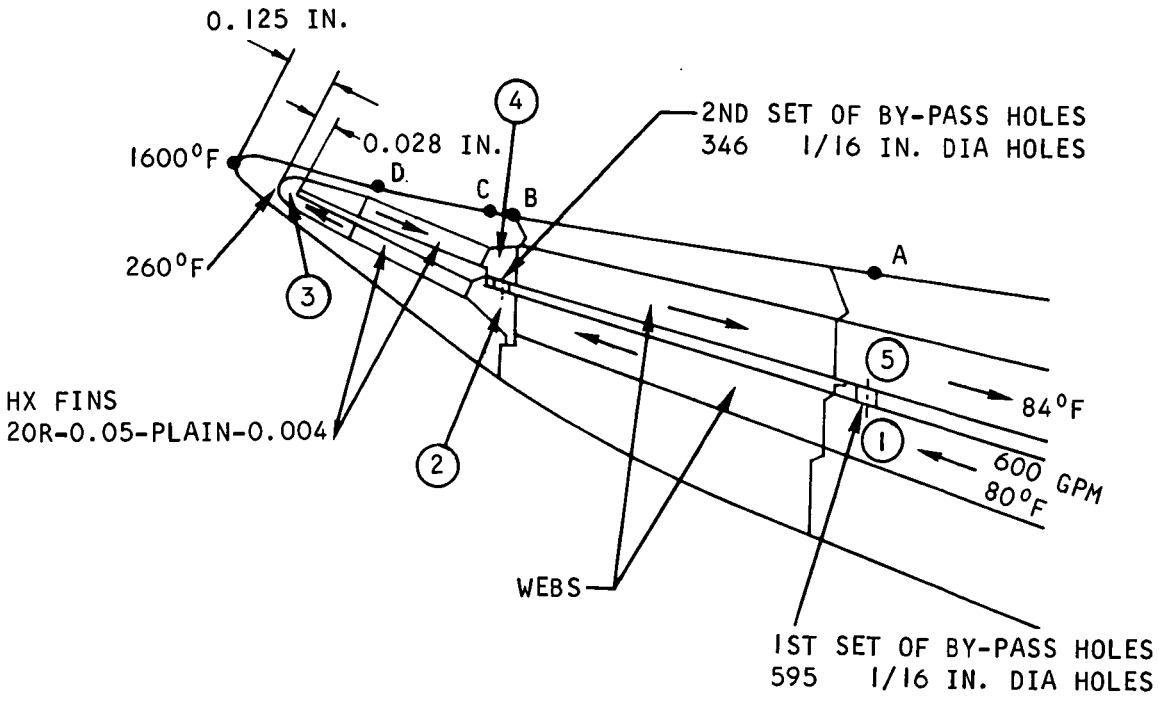

NOTES

1. FLOW DISTRIBUTION

   $\dot{w}_{H_2O}$ (①) = 660 GPM

   (① → ②) = 340 GPM
   (① → ⑤) = 320 GPM: 1ST BY-PASS HOLES
   (② → ③ → ④) = 170 GPM
   (② → ④) = 170 GPM: 2ND BY-PASS HOLES

2. PRESSURE DROP

   Δp (① → ⑤) = 49 PSI
   Δp (② → ③ → ④) = 41 PSI

3. WALL TEMPERATURES WHEN THE SPIKE COMPRESSION WAVES IMPINGE ON THE RESPECTIVE LOCATIONS:

Point	Heat Flux, Btu/sec ft^2	Wall Temperatures, °F	
		Gas Side	Coolant Side
A	543	1020	350
B	608	748	360
C	595	800	262
D	661	520	278

4. GAS CONDITIONS

   $M_\infty = 6.65$, $p_{T_\infty} = 1200$ PSIA, $T_{T_\infty} = 3770°R$

Figure 5-7. Tip Section of Outerbody Leading Edge - Nickel Walls

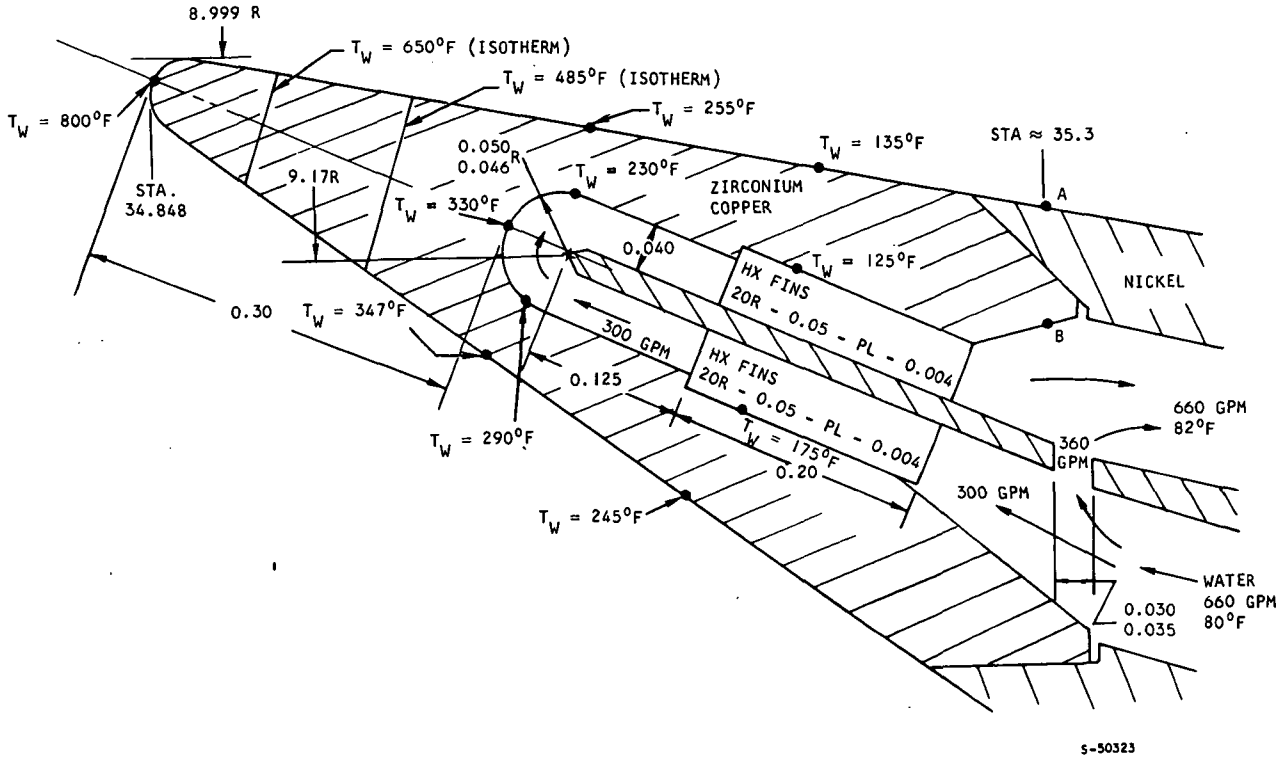

NOTES

1. DIMENSIONS IN INCHES
2. GAS CONDITIONS: $M_\infty = 6.65$, $P_{T_\infty} = 1200$ PSIA, $T_{T_\infty} = 3770°R$
3. SPIKE SHOCK IMPINGEMENT EFFECTS:
   $\frac{h(Peak)}{h(F\text{-}R)} = 10$, $h(Peak) = 0.171 \times 10 = 1.71$ Btu/sec/ft^2-°F
   $\Delta X(\text{Peak Heating Width}) = \frac{.2r_o}{20} = 0.003$ in.
   h(F-R) = Fay-Riddell Stagnation Heat Transfer Coefficient with Spike Shock Inside Cowl Lip
4. MULTIPLICATION FACTOR DUE TO UPSTREAM AIR TURBULENCE EFFECT ON STAGNATION COEFFICIENT EXCEPT PEAK HEATING ZONE = 1.8 (REF. 5-5).
   h_{STAG} = 0.171 x 1.8 = 0.308 Btu/sec ft^2-°F WITH SPIKE SHOCK INSIDE COWL LIP
   = 0.278 x 1.8 = 0.50 Btu/sec ft^2-°F WITH SPIKE SHOCK OUTSIDE COWL LIP
5. MULTIPLICATION FACTOR DUE TO CURVATURE ON COOLANT COEFFICIENT = 1.55 (REF. 5-5).
   COOLANT HEAT TRANSFER COEFFICIENT AT IMPINGING POINT = 6.2 Btu/sec ft^2-°F
6. WHEN COMPRESSION WAVES FROM SPIKE COMPRESSION CORNER IMPINGES ON STATION = 35.3, $T_A = 620°F$, $T_B = 360°F$ (ONE-DIMENSIONAL ANALYSIS)
7. $(\Delta p)_{WATER} \cong$ 50 PSI IN REGION SHOWN
8. THERMAL CONDUCTIVITY OF ZIRCONIUM-COPPER = 198 Btu/hr-ft^2-°F (REF. 5-6).

Figure 5-8. Cooling of Outerbody Leading Edge Tip - Zirconium-Copper Tip

The zirconium-copper considered, contains 0.1 to 0.2 percent of zirconium, and has a high thermal conductivity of 198 Btu/hr ft ^{0}F (Reference 5-6), which is close to that of OFHC copper of 210 Btu/hr ft ^{0}F. Therefore, this change of the tip material has a minor effect on the heat conduction pattern in the tip. The temperature distribution in the zirconium-copper tip, shown in Figure 5-8, includes the effects of upstream flow turbulence and spike shock impingement.

The sides of the leading edge are well cooled by the present cooling system (Figure 5-8). At a location in the internal gas flow passage where the compression waves from the spike compression corner may impinge, however, a localized peak-heating is expected. The location of this peak-heating is between Stations 36 and 39 for the M_{∞} = 6.65 gas conditions. The magnitude of peak-heating and associated cooling conditions were reported in Reference 5-4. If this peak-heating due to impingement of spike compression waves occurs at Station 35.3, where the coolant flow velocity is minimum, the temperatures shown in Figure 5-8 may result (Points A and B).

Due to space limitations in this area for the cooling water, a large coolant pressure drop would result if the total water flow rate of 660 gpm were to flow through the tip-cooling passage. Since a water flow rate of about 300 gpm is calculated to be needed to cool the tip section, a bypass is provided for the remaining 360 gpm. A pressure drop of about 50 psi is estimated in this region.

5.3.2 Spike Tip

The material of the spike tip was changed from OFHC-copper to zirconium-copper for a structural reason and is shown in Drawing No. 950512 (attached at the end of this report). The spike tip is cooled by the water impinging on the back surface of the zirconium-copper piece. Three-dimensional analysis predicts that the zirconium-copper stagnation point temperature is 966^{0}F, with the stagnation heat flux of 380 Btu/sec ft^{2} which was calculated from the Fay-Riddell equation for the M_{∞} = 6.65 gas conditions. In this case, the average water-wetted back side wall temperature is 270^{0}F.

In Reference 5-5, it was reported that the effect of upstream turbulence on the heat transfer rate near a stagnation region can be significant depending on turbulence intensity. For the tip of the outerbody leading edge, a multiplication factor of 1.8 was used to account for this effect. When the same multiplication factor of 1.8 due to upstream turbulence is applied to the spike tip, a zirconium-copper stagnation point temperature of 1148^{0}F is calculated, with the stagnation heat flux of 632 Btu/sec ft^{2} and the average water-wetted back side wall temperature of 285^{0}F for the M_{∞} = 6.65 gas conditions (three-dimensional analysis).

5.3.3 Fuel System

The fuel injector manifolds, shown for the outer shell in Drawing L-950991 were designed for a ratio of maximum-to-minimum injector hole flow of 1.04 or less. The table below indicates the design conditions, manifold inside diameters and calculated maximum-to-minimum flow ratios.

The maximum required hydrogen inlet pressure at the HRE/AIM-facility interface is 500 psia.

	Fuel Manifold and Location						
Parameter	1A Spike	1B Outer Shell	2A Outer Shell	2B Outer Shell	3A Outer Shell	3B Inner Shell	4 Outer Shell
Fuel manifold pressure, psia	200	200	310	310	370	370	250
Fuel manifold temperature, ^{o}R	1500	1500	1500	1500	1500	1500	1500
Flow, lb/sec	0.32	0.32	0.30	0.63	0.75	0.75	0.30
Manifold diameter, in.	0.902	0.902	0.712	0.962	0.902	0.777	1.05
W_{max}/W_{min}	1.022	1.022	1.02	1.027	1.033	1.015	1.007
Injector area, $in.^2$	0.754	0.754	0.442	0.93	0.94	0.94	0.563
Manifold area, $in.^2$	1.28	1.28	0.796	1.45	1.28	1.9	1.73
Inlet tube min area, $in.^2$	0.91	0.91	0.53	1.11	1.13	1.13	0.677

6. DESIGN AND FABRICATION

The design activity expended during this reporting period was directed towards (1) completing the layout drawing of the outer shell; (2) completing the major weldment drawings of the inner shell, outer shell, and the outer cowl; and (3) design modification associated with redesign of the cowl leading edge and incorporation of the IC injector into the inlet spike assembly.

6.1 SUBASSEMBLY STATUS

6.1.1 Inlet Spike

Design modification incorporating the IC fuel injector and the zirconium-copper tip was released to manufacturing. The area between fuel injector IA and the skirt assembly was completely redesigned to incorporate the IC injector. This area was originally allocated for instrumentation equipment and the transition of items affixed to the spike. The incorporation of the IC injector in an already-confined area created a difficult task of packaging, fabricating, and assembling the spike assembly.

6.1.2 Inner Shell (950984)

The major components of the inner shell have been released to manufacturing and detail parts are now being machined.

The spike actuator housing is now being chromium plated. Upon completion of this operation the actuator will be installed and functionally tested.

6.1.3 Nozzle Plug (950988)

The assembly of the nozzle plug is continuing. The nickel (hot) shell is being assembled to the inner shell. No additional problems in welding are anticipated since all remaining welds are to be made on like materials. The nozzle plug is now scheduled to be completed by the end of August with the exception of the final contour-machining. The final contouring will be completed at the same time the final contour is machined on the inner shell.

6.1.4 Cowl Leading Edge (950986)

The drawing incorporating the zirconium-copper tip has been released to manufacturing. Areas not affected by this redesign are progressing as scheduled. The zirconium-copper forging is scheduled to be available for machining 11 July 1969. Test specimens to define welding procedure have been ordered and tests will be performed during the next reporting period.

6.1.5 Outer Shell and Engine Support Struts

The nickel hot shell has been welded and is now being machined for fit-up in the first brazed assembly. All of the fin material is on hand ready to be fitted to the nickel shell. Problems were encountered in rolling the shells and maintaining roundness; also, a delay was encountered in the delivery of the Hastelloy X shells, and they are now due during the week of 23 June 1969.

6.1.6 Nozzle Shroud (950987)

The assembly of the nozzle shroud is continuing, and the anticipated completion date is the end of August. This date does not include the machining of the final contour, which will be cut on the nozzle shroud at the same time as the outer shell and the cowl leading edge.

6.1.7 Outer Cowl and Engine Support Strut Fairing

The detail drawings have been released to manufacturing, and machining of some of the detail parts has been initiated. Difficulties encountered in release of these drawings was due to problems related to establishing manufacturing procedures so that the tolerances of the finished parts would satisfy requirements of stress analysis and heat transfer.

PN 950529 manifold assembly, which links the coolant system between the two halves of the outer cowl assembly, was completed.

6.1.8 Inner Shell/Outer Shell Support Struts (950983)

All of the detail parts and subassemblies that fit through the struts have been completed and are now on hand, with the exception of the lines smaller than 1/2 in. dia. These lines will be formed during the assembly of the engine. The final machining of the struts to fit the sockets will be completed during the engine buildup.

6.1.9 Combustor Exit and Nozzle Exist Instrumentation

Layout drawing for the combustor exit and the nozzle exit was initiated. The design will be completed during the next reporting period.

6.1.10 Igniter Assembly and Associated Components

Igniter assembly similar to that used on the initial HRE test program, performed at Ordinance Aerophysices Laboratory, Daingerfield, Texas, was designed and fabricated. PN PA106753 (drawing attached at end of this report) was assigned to this unit for initial test purpose (Figures 6-1, 6-2, and 6-3).

The unit has been subjected to tests, and definition of energy required to initiate combustion has been established utilizing a variable energy excitor unit manufactured by General Laboratories Associate of Norwich, New York.

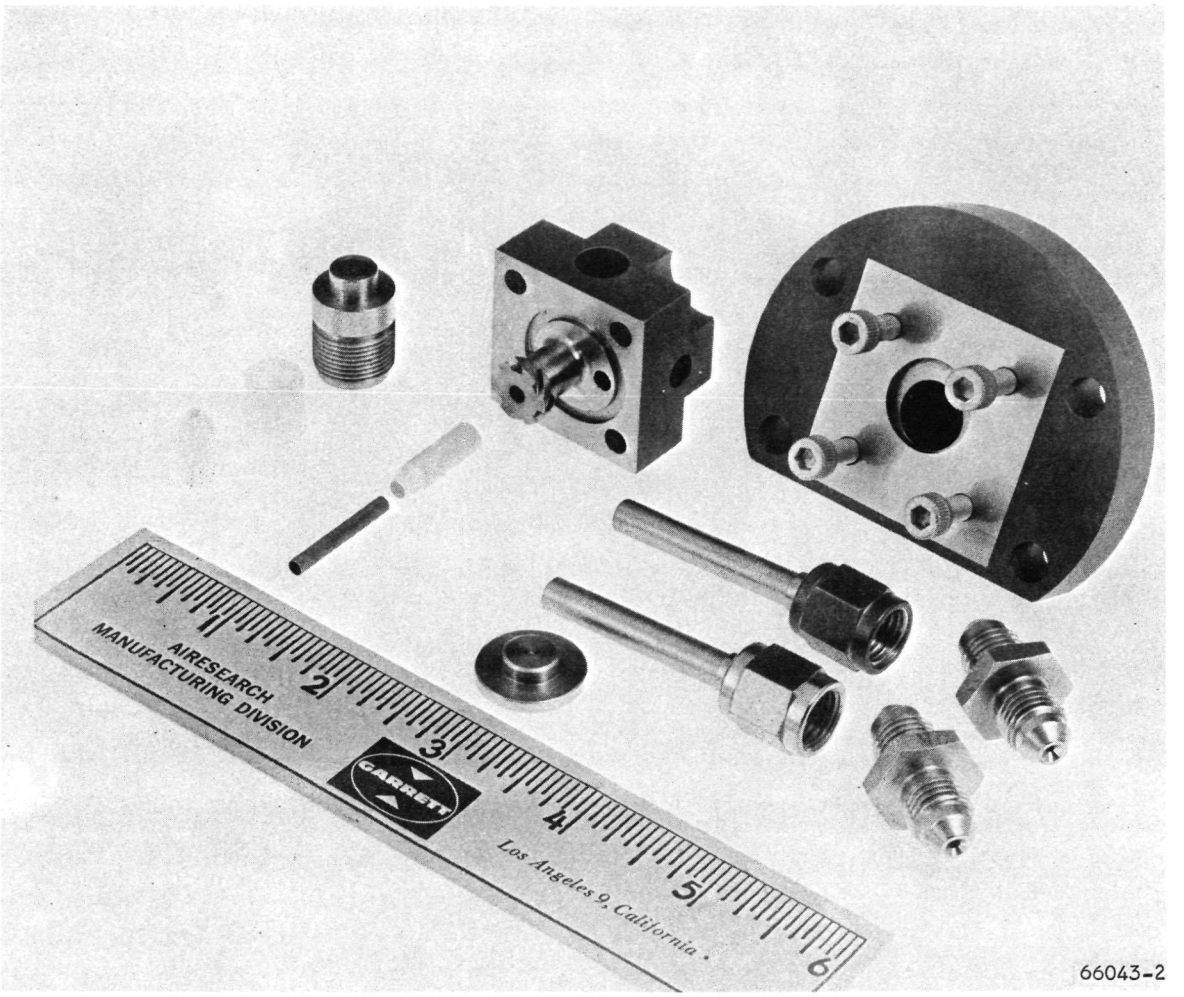

Figure 6-1. Igniter Assembly, Diassembled

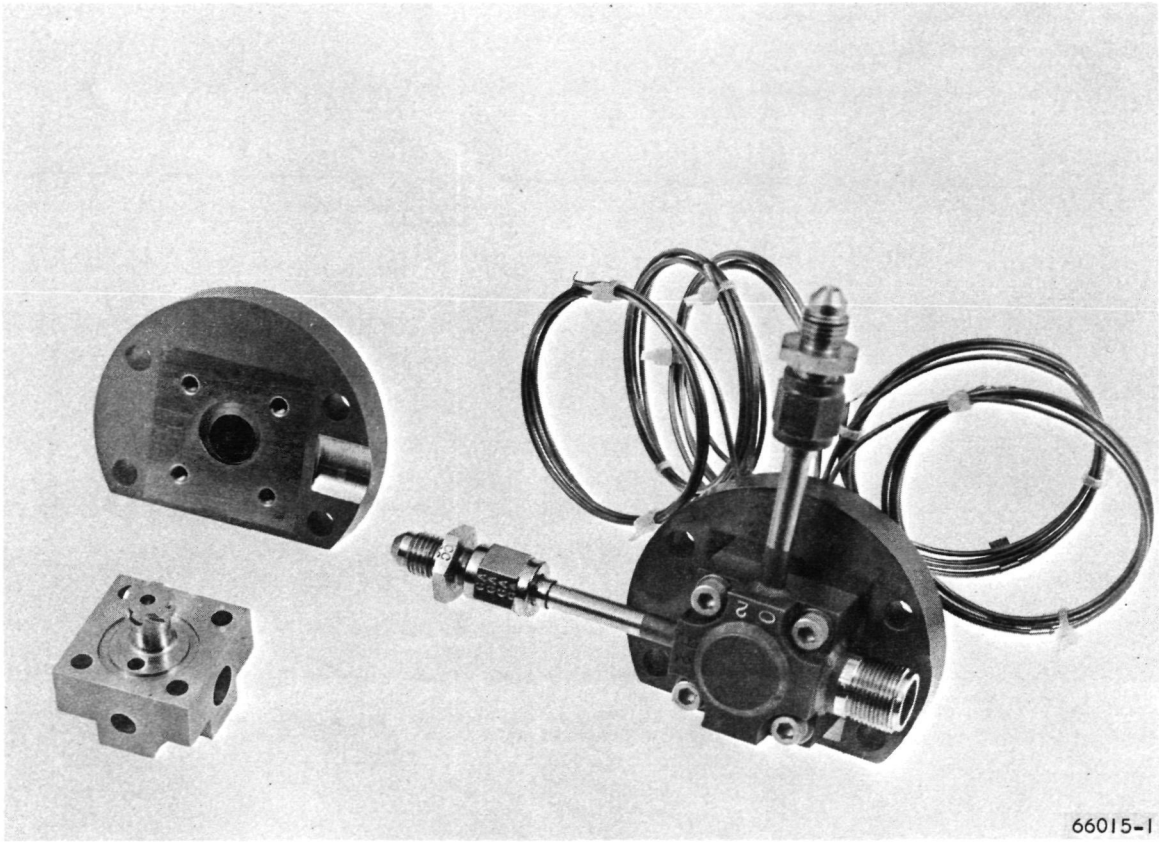

Figure 6-2. Igniter Assembly, Rear View

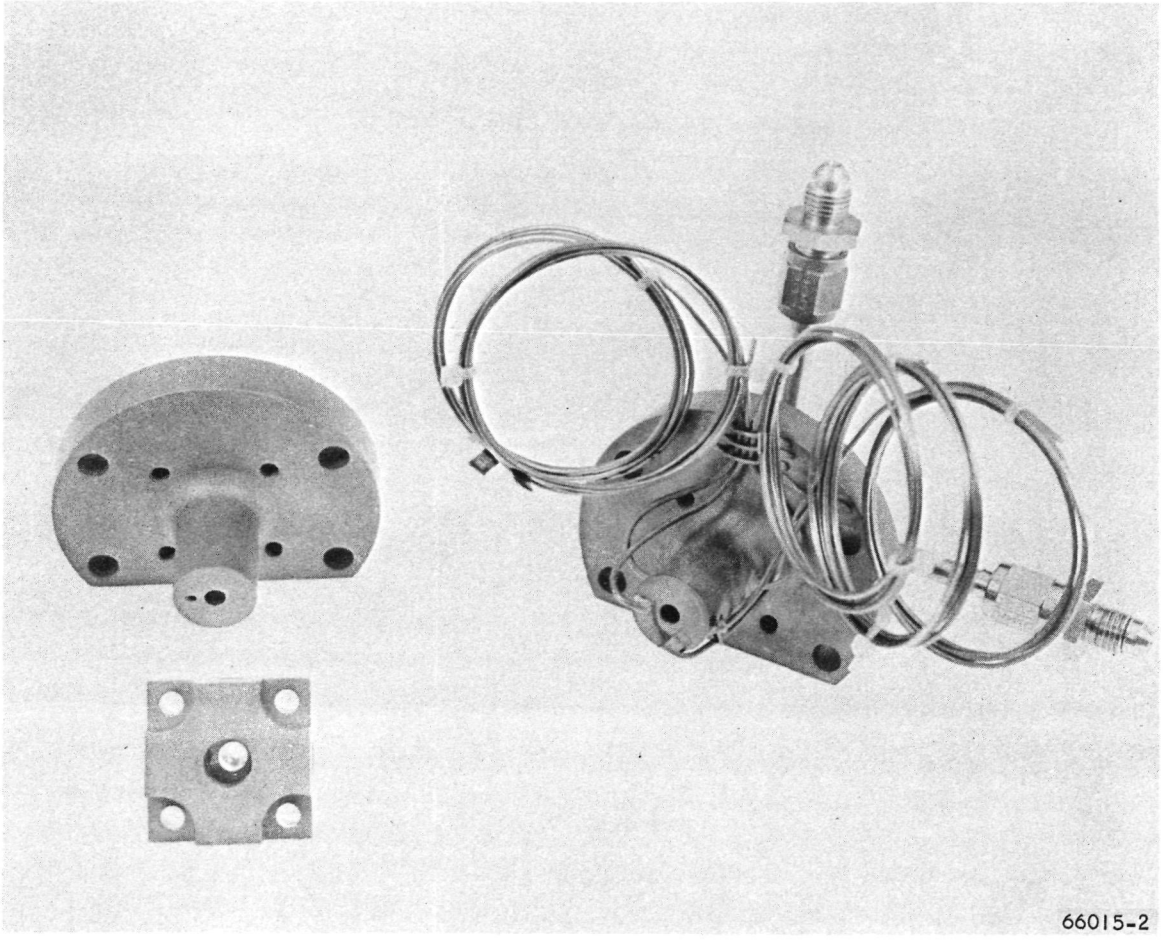

Figure 6-3. Igniter Assembly, Front View

Tests were performed at an oxygen-hydrogen fuel ratio of 8 to 1 and 5 to 1 for a combustion chamber pressure range of 50 psig to 250 psig. The energy required to ensure ignition of this mixture was established as 0.02 joules.

Tests to establish endurance limits and operating envelope will be performed during the next reporting period.

7. FUTURE ACTION

7.1 DESIGN ACTIVITY

All detail drawings for the AIM will be completed by 18 July 1969, and the final assembly drawing is scheduled for completion on 1 August 1969.

Design of the combustor exit and nozzle exit instrumentation will be completed during the next reporting period.

Configuration of the fuel injectors will be defined upon completion of the two-dimensional combustor test presently in process.

7.2 TESTS

Igniter assembly will be subject to further testing to establish endurance level and to determine operational range.

Tests will be performed to establish welding schedules to join zirconium-copper to Nickel-200.

REFERENCES

5-1 De Marquis, D. Wyatt, "Analysis of Errors Introduced by Several Methods by Weighting Nonuniform Duct Flows," NACA TN3400.

5-2 Engineering Staff, Hypersonic Research Engine Project - Phase IIA, Third Oral Review Technical Presentation (U), AiResearch Report AP-68-4276, Data Item No. 56-03T, 16 October 1968, CONFIDENTIAL.

5-3 Engineering Staff, Hypersonic Research Engine Project - Phase IIA, Phase IIA Boilerplate Engine Development Second Interim Technical Data Report (U), Data Item No. 55-4.02, AiResearch Report No. AP-68-4285, 11 October 1968, CONFIDENTIAL.

5-4 Engineering Staff, Hypersonic Research Engine Project - Phase IIA, Phase IIA Aerothermodynamic Integration Model (AIM) Development, Fourth Interim Technical Data Report, Data Item No. 55-4.04, AiResearch Report No. AP-69-4932, 15 April 1969.

5-5 Engineering Staff, Hypersonic Research Engine Project - Phase IIA, Phase IIA Boilerplate Engine Development, Third Interim Technical Data Report(U), Data Item No. 55-4.03, AiResearch Report No. AP-69-4674, 24 January 1969, CONFIDENTIAL.

5-6 American Metals Climax, Inc., "AMZIRC, High-Conductivity Zirconium-Copper with High Strength at Elevated Temperatures," Technical Data Report.

APPENDIX A

INLET-COMBUSTOR INTERACTION MODEL ANALYSIS

APPENDIX A

INLET-COMBUSTOR INTERACTION MODEL

The flow model for inlet-combustor interaction is as shown below:

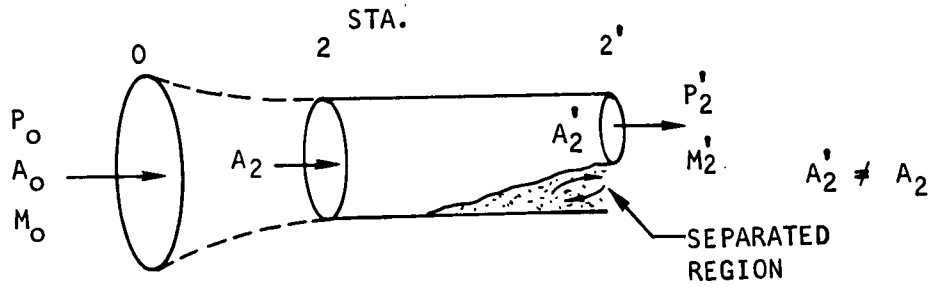

$$F_2 = F_2' \quad \text{and since} \quad \dot{w}_o = \dot{w}_2 = \dot{w}_2'$$

$$F_2 = P_2' A_2 + \frac{\dot{w}_2 V_2'}{g} \qquad \text{(Pressure term applies to entire area; zero flow assumed in separated region)}$$

Dividing by $P_2 A_2$ and rearranging:

$$\frac{P_2'}{P_2} = \frac{F_2}{P_2 A_2} - \frac{\dot{w}_2 V_2'}{P_2 A_2 g}$$

For an ideal gas

$$\dot{w}_2 = \frac{\left(P/P_t \dot{m}\right)_o P_{t_o} A_o}{\sqrt{T_{t_o}}}$$

$$\frac{P_2'}{P_2} = \frac{F_2/P_o A_2}{P_2/P_o} - \frac{\left(P/P_t \dot{m}\right)_o A_o P_{t_o}/P_o V_2'}{\sqrt{T_{t_o}} P_2/P_o A_2 g}$$

or

$$\frac{P_2'}{P_2} = \frac{1}{P_2/P_o}\left[\frac{F_2}{P_o A_2} - \frac{\left(P/P_t \dot{m}\right)_o A_o/A_2 V_2'}{\sqrt{T_{t_o}} \left(P/P_t\right)_o \times g}\right] \qquad \text{(A-1)}$$

Thus the pressure rise (P_2'/P_2) can be found versus M_2' (or V_2') once inlet conditions such as $F_2/P_o A_2$, P_2/P_o and A_o/A_2 are known.

The parameter $\frac{F_2}{P_o A_2}$ was obtained by integrating the pitot profiles at the inlet throat as shown in Figures A-1 and A-2.* The value of P_2/P_o was calculated using the mass-momentum technique as follows:

From continuity,

$$\dot{w}_2 = \dot{w}_o$$

or $$\frac{P_2 A_2 \dot{m}_2}{\sqrt{T_{t_2}}} = \frac{\left(P/P_t\ \dot{m}\right)_o P_{t_o} A_o}{\sqrt{T_{t_o}}}$$

where $\dot{m} = \dot{W}\sqrt{T_t}/PA$

since $F_2 = P_2 A_2\left(1 + \gamma M_2^2\right)$ and dividing both sides by F_2

$$\therefore \quad \frac{\dot{m}_2}{\left(1 + \gamma M_2^2\right)} = \frac{\left(P/P_t\ \dot{m}\right)_o P_{t_o}}{F_2} A_o \sqrt{\frac{T_{t_2}}{T_{t_o}}}$$

Multiply both sides by $\sqrt{\frac{R}{\gamma g}}$

$$\dot{m}_2 \left(1 + \gamma M_2^2\right)^{-1} \sqrt{\frac{R}{\gamma g}} \frac{\left(P/P_t\ \dot{m}\right)_o P_{t_o}}{F_2} A_o \sqrt{\frac{T_{t_2}}{T_{t_o}}} \sqrt{\frac{R}{\gamma g}}$$

Since $$N_2 = \frac{\left(P/P_t\ \dot{m}\right)_o A_o/A_2}{\frac{F_2}{P_o A_2}\left(P/P_t\right)_o} \sqrt{\frac{R}{\gamma g}} \sqrt{\frac{T_{t_2}}{T_{t_o}}} \qquad \text{(A-2)}$$

M_2 can be easily obtained from tables. Also

$$\frac{F_2}{P_o A_2} = P_2 A_2 \left(1 + \gamma M_2^2\right) \quad \text{and} \quad \frac{P_2}{P_o} = \frac{F_2/P_o A_2}{\left(1 + \gamma M_2^2\right)}$$

---

*Engineering Staff, Hypersonic Research Engine Inlet Development Program - Wind Tunnel Test Summary Report, Lockheed Aircraft Company Report LR 22071, December 1968.

	GROUP	Re/FT	α	X_L, IN.	$\bar{T}_W/T_{To}$	CR
M_o = 6.05	244	4.04×10^6	-0.30°	23.28	0.508	8.45

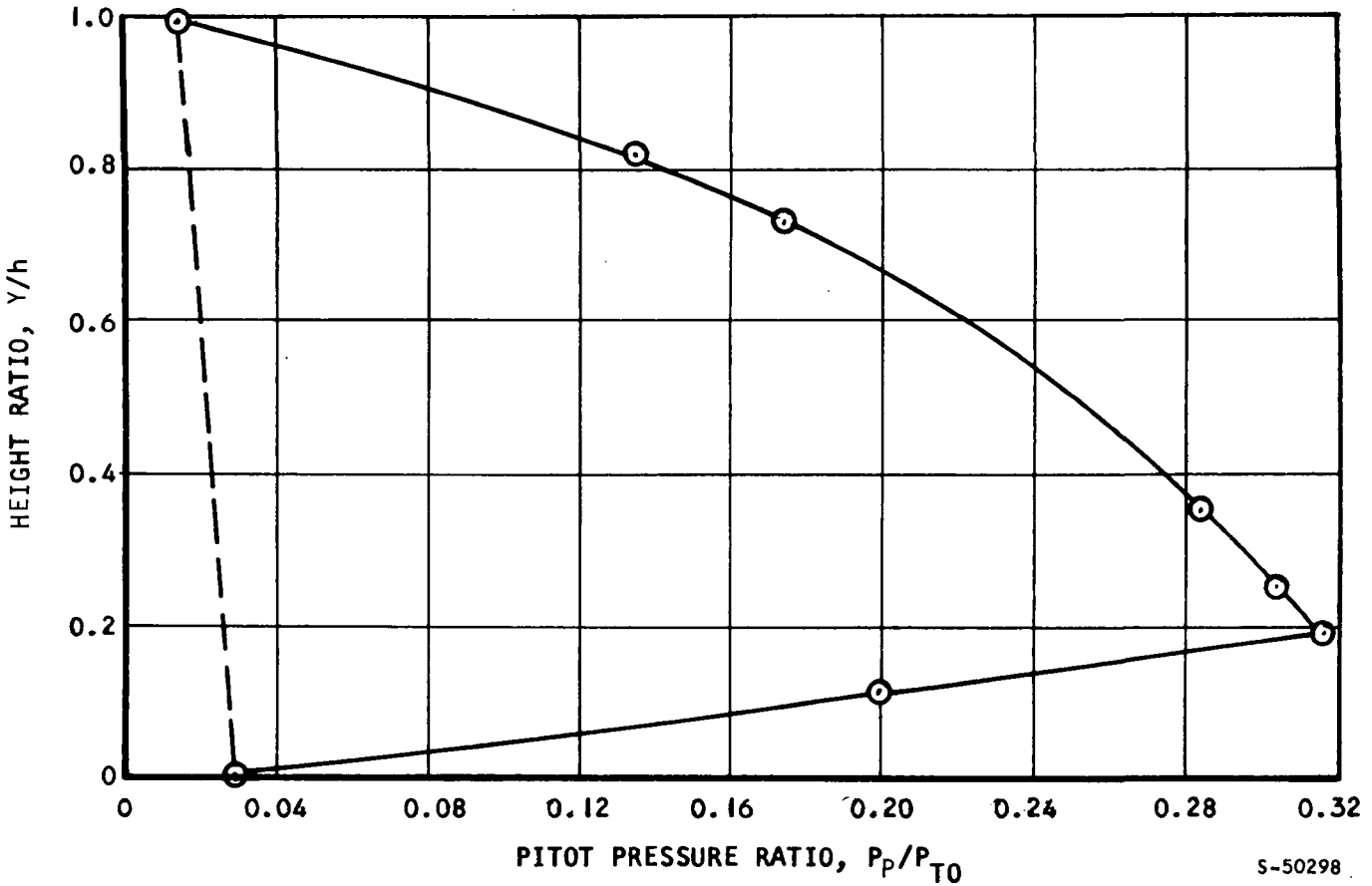

Figure A-1. Pitot Pressure Profiles, M_o = 6.05

	GROUP	Re/FT	α	X_{CL}, IN.	X_P	$\bar{T}_W/T_{To}$	CR
M_o = 8.0	234	2.87×10^6	0.0	24.56	1.59	0.399	13.62

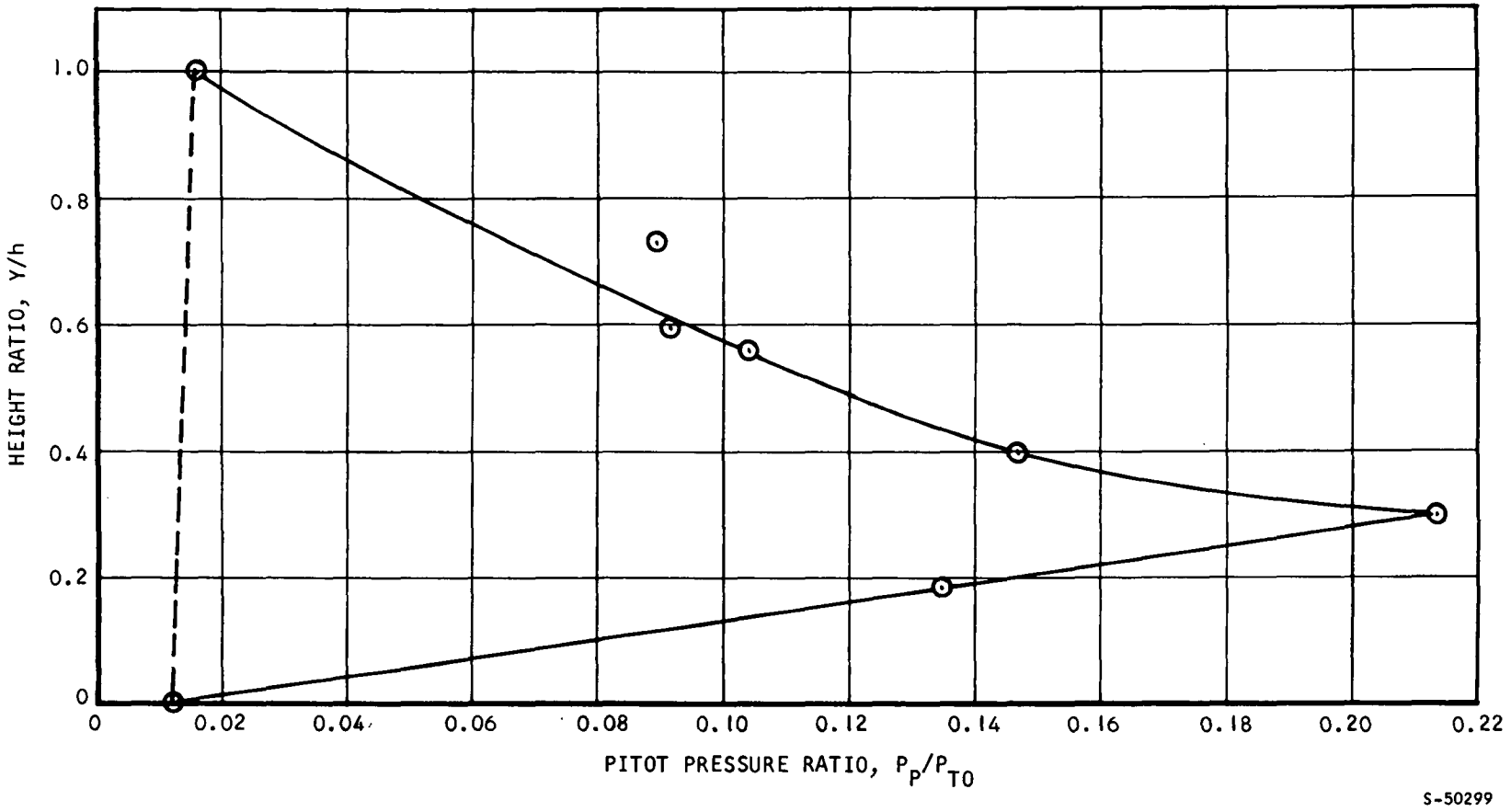

Figure A-2. Pitot Pressure Profiles, M_o = 8.0

Also $$\frac{P_{t_2}}{P_{t_o}} = \frac{P_2/P_o \left(P/P_t\right)_o}{\left(P/P_t\right)_2}$$

The pitot profiles were integrated to obtain the following:

M_o	A_o/A_2	T_{t_2}/T_{t_o}	F_2/P_oA_2	T_{t_o}, °R
6.05	8.45	0.955	370	850
8	13.62	0.95	1097	1250

For Mach 8 using Equation (A-2)

$$N_2 = \frac{0.0027972(13.62)}{1097(0.00010243)} \sqrt{\frac{R}{\gamma g}} \sqrt{0.95}$$

$$N_2 = 0.35945 \quad \therefore \quad M_2 = \underline{3.43}$$

$$P_2/P_o = \frac{1097}{17.48} = \underline{62.8}$$

$$P_{t_2}/P_{t_o} = 62.8 \frac{(0.00010243)}{0.0144875} = \underline{0.45}$$

For Mach 6.05

$$N_2 = \frac{0.0096511(8.45)}{370(0.00060183)} \sqrt{\frac{R}{\gamma g}} \sqrt{0.955}$$

$$N_2 = 0.38946 \quad \therefore \quad M_2 = 2.374$$

$$P_2/P_o = \frac{370}{8.8902} = \underline{41.6}$$

$$P_{t_2}/P_{t_o} = \frac{41.6(0.00060183)}{0.071234} = 0.35$$

For each assigned value of M_2', using Equation (A-1), two curves were obtained at Mach 6 and 8 as shown in Figure 5-1 (main text).

The mass momentum averaged pressure recoveries were used to obtain engine performance.

APPENDIX B

CONVERSION OF IDEAL GAS TEST RESULTS

APPENDIX B

CONVERSION OF IDEAL GAS TEST RESULTS

The pressure rise to unstart the inlet from test data was 2.3 at Mach 6 and 3.0 at Mach 8. These results were for an ideal gas. For the real gas case, the following procedure was used:

Using the same model as Appendix A

$$F_2 = P_2A_2 + \dot{W}_2 \frac{V_2}{g} = P_2'A_2 + \dot{W}_2' \frac{V_2'}{g}$$

$$\frac{P_2'}{P_2} = 1 + \frac{\dot{W}_2}{P_2A_2} \frac{V_2}{g} - \frac{\dot{W}_2'}{P_2A_2} \frac{V_2'}{g}$$

Since $\dot{W}_2' = \dot{W}_2 = \dot{W}_o = \rho_o V_o A_o$

$$\frac{P_2'}{P_{2_{R.G.}}} = 1 + \frac{\rho_o V_o^2 A_o/A_2}{P_o (P_2/P_o) g} \left[\frac{V_2}{V_o} - \frac{V_2'}{V_o} \right] \qquad \text{(B-1)}$$

Using the results from Appendix A

M_o	$P_{t_2}/P_{t_o}{}_{R.G.}$	A_o/A_2	$P_2/P_o{}_{R.G.}$	$M_{2_{R.G.}}$
6.0	0.35	8.35	42.5	2.32
8	0.46*	14.2	68	3.62

*This value is 2 percent higher than the inlet test total pressure recovery because of the change in A_o/A_2 (14.2 vs test value of 13.62).

M_o	$V_2/V_o{}_{R.G.}$	M_2'	$V_2'/V_o{}_{R.G.}$
6.0	0.775	1.7	0.62
8	0.87	2.42	0.728

Substituting the above values into Equation (B-1) gives:

M_o	P_2'/P_2 ideal gas	P_2'/P_2 real gas
6	2.3	2.64
8	3	3.97

UNCLASSIFIED

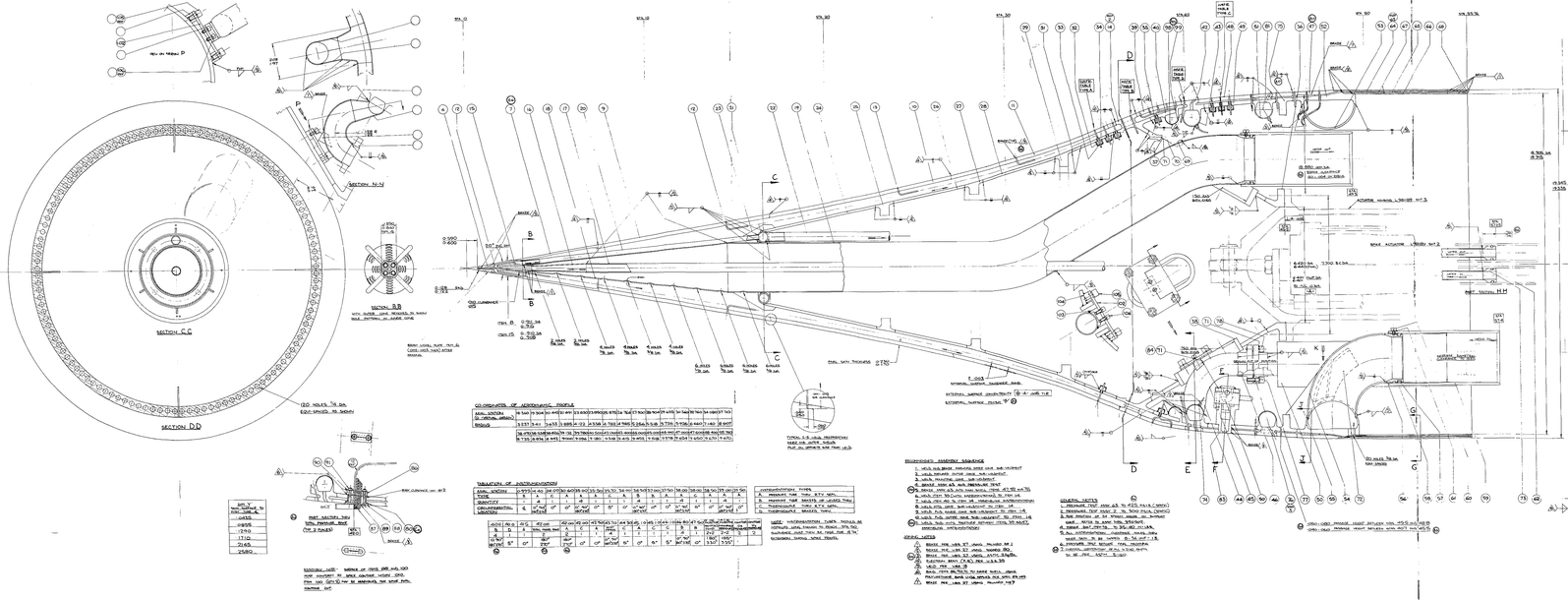

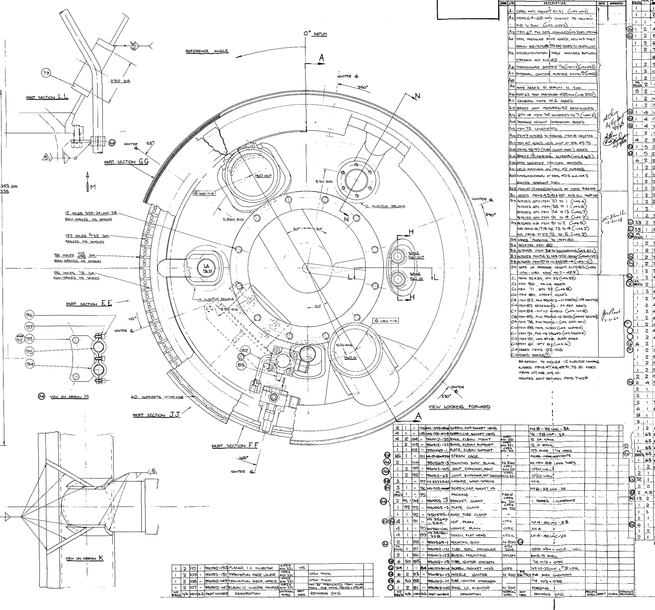

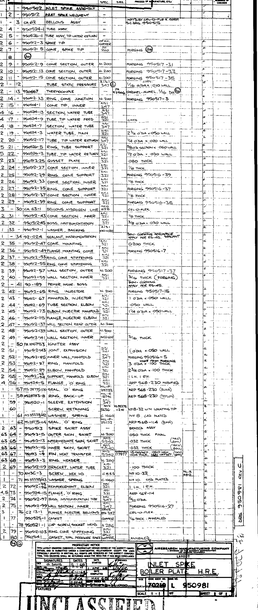

UNCLASSIFIED

UNCLASSIFIED

STA	θ DIR	REMARKS
42.140	90°	STATIC PRESS, HOT GAS
42.140	90°	TOTAL PRESS,
42.140	90°	↓
42.140	90°	↓
42.140	90°	↓
42.140	90°	TOTAL PRESS,
42.140	180°	STATIC PRESS,
42.140	180°	TOTAL PRESS,
42.140	180°	↓
42.140	180°	↓
42.140	180°	TOTAL PRESS,
43.810	1°	STATIC PRESS,
43.810	90°	↓
43.810	180°	↓
43.810	270°	↓
46.250	1°	↓
47.000	1°	↓
49.000	1°	↓
49.000	90°	↓
49.000	180°	↓
49.000	270°	↓
49.500	0°	↓
50.400	0°	↓
50.400	90°	↓
50.400	180°	↓
50.400	270°	↓
51.500	1°	↓
52.500	0°	↓
53.000	1°	↓
53.000	90°	↓
53.000	180°	↓
53.000	270°	↓
54.500	0°	↓
56.500	0°	↓
57.500	0°	↓
58.500	0°	↓
59.500	0°	↓
60.500	0°	↓
61.900	0°	↓
61.900	110°	↓
61.900	180°	↓
61.900	290°	↓
63.900	0°	↓
64.000	0°	↓
65.000	1°	STATIC PRESS, HOT GAS
42.000	0°	TEMPERATURE, HOT SKIN
42.500	0°	↓
43.810	359°	↓
45.750	359°	↓
46.600	0°	↓
46.500	90°	↓
46.500	180°	↓
46.500	270°	↓
47.000	359°	↓
49.000	359°	↓
50.000	0°	↓
50.000	90°	↓
50.000	180°	↓
50.000	270°	↓
51.500	359°	↓
52.000	0°	↓
53.000	359°	↓
56.000	0°	↓
56.000	120°	↓
56.000	240°	↓
57.000	0°	↓
58.000	0°	↓
59.000	0°	↓
60.000	0°	↓
61.000	0°	↓
62.500	0°	↓
62.500	120°	↓
62.500	240°	↓
63.500	0°	↓
64.500	0°	↓
65.250	359°	TEMPERATURE, HOT SKIN

ITEM	POINT NO.	STA	Y	Z	REMARKS
29	1	48.810	-11.515	0.000	INTERSECTION OF ITEM 30 & INTER. ITEM 28
	2	50.650	-12.585	0.000	MOLD POINT
	3	53.625	-12.880	0.000	MOLD POINT
	4	53.625	-12.470	-2.495	E.O.P.

TUBE BEND RADIUS = 1.00

ITEM	POINT NO.	STA	Y	Z	REMARKS
30	1	48.810	-11.183	6.980	INTERSECTION OF ITEM 30 & INTER. ITEM 28
	2	50.650	-12.156	3.257	MOLD POINT
	3	53.625	-12.441	3.334	↓
	4	53.625	-11.566	6.678	↓
	5	53.000	-13.549	7.823	MOLD POINT
	6	53.000	-13.881	8.020	E.O.P.

TUBE BEND RADIUS = 1.00

ITEM	POINT NO.	STA	Y	Z	REMARKS
207	1	53.625	-12.425	-2.715	E.O.P.
	2	53.625	-11.696	-6.753	MOLD POINT
	3	53.000	-13.722	-7.973	MOLD POINT
	4	53.000	-13.891	-8.060	E.O.P.

TUBE BEND RADIUS = 1.00

ITEM	POINT NO.	STA	Y	Z	REMARKS
52	1	43.746	-9.651	5.595	INTERSECTION OF ITEM 53 & INTER. ITEM 54
	2	45.030	-9.520	6.176	M.P. BEND R=1.00
	3	45.975	-10.390	6.421	M.P. BEND R=3.50
	4	47.325	-12.680	7.320	M.P. BEND R=1.00
	5	47.325	-15.100	8.720	SURFACE ITEM 57

ITEM	POINT NO.	STA	Y	Z	REMARKS
33	1				
	2	45.030	-9.520	-6.176	M.P. BEND R=1.00
	3	45.975	-10.990	-6.421	M.P. BEND R=3.50
	4	47.325	-12.680	-7.32	M.P. BEND R=1.00
	5	47.325	-15.100	-8.720	SURFACE ITEM 41

AERODYNAMIC CONTOUR

STA	40.500	40.894	41.894	42.894	43.894	44.294	55.740	57.000	58.000	58.700	61.900	65.740	65.997	66.246	66.512
R	9.4950	9.7300	9.8100	9.8900	9.9550	10.1320	10.6725	10.9550	11.0000	11.0150	11.0150	11.0150	11.0250	11.0480	11.0810

✦ RUNOUT

ZONE	LTR	REVISIONS DESCRIPTION	DATE	APPROVED

ITEM	QTY PER	NEW	OLD	PART NUMBER	DESCRIPTION	MATERIAL	REF.	REMARKS (HEAT TREATING, PLATING PROCESS OF MANUFACTURE, ETC.)	SPEC.	DRAFT.	CHECK.	APPROVAL NUMBERS OF CHECKERS
166	1	167		950G52-1	TUBE ASSY, MID, H_2 IGNITOR							
167	1	168		-3	TUBE	CRES AISI 321		3/16 O.D. - .028 WALL				
167	1	169		-5	FITTING			CODE 9 FOR 3/16 TUBE PARKER HANNIFIN				
1	1	170		950G00-11	MANIFOLD, END, N_2 IGNITOR							
170	1	171		950G53-1	TUBE ASSY, END, H_2 IGNITOR							
171	1	172		-5	TUBE	CRES AISI 321		3/16 O.D. - .028 WALL				
171	1	173		-5	CAP	CRES AISI 321		.032 SHEET				
1	6	174		950G57-1	TUBE ASSY, EXIT, H_2							
174	1	175		-3	TUBE	CRES AISI 321		3/16 O.D. - .020 WALL				
174	1		170	AN818-4C	NUT							
174	1		177	MS20819-4C	SLEEVE							
1	6		178	S9026A019	PACKING, O-RING							
1	68		179	MS35338-45	WASHER, LOCK							
1	24		180	NAS1351-3H4	SCREW							
1	4		181	NAS1351-5LE8P	SCREW							
1	18		182	NAS1351-5LE8P	SCREW							
1	22		183	NAS1351-3LE4P	SCREW							
1/64	1		184	5-BZ-SS	NUT			PARKER HANNIFIN AIRA TEMP. 200LV COATING PARKER HANNIFIN				
1/32	1		185	5-TZ-SS	FERRULE			AIRA TEMP. 200LV COATING PARKER HANNIFIN				
1/64	1		186	6-BZ-SS	NUT			AIRA TEMP. 200LV COATING PARKER HANNIFIN				
1/64	1		187	6-TZ-SS	FERRULE			AIRA TEMP. 200LV COATING				
9	6		188	950G35-15	SOCKET	MAT'L AMS 5541		.050 SHEET				
—	1		189	950G54-1	SPACER	MAT'L AMS 5511		.040 SHEET				
—	1		190	950G54-2	SPACER	MAT'L AMS 5511		.040 SHEET				
59	1		191	950G16-1	FORGING,	MAT'L AMS 5754						
1/4	1/8		192	950G16-2	FORGING	MAT'L AMS 5754						
67	1		193	950G17-1	FORGING	N-200						
1/8	1		194	950G18-1	FORGING	CRES AISI 347						
1/64	1		195	950G18-2	FORGING	CRES AISI 347						
5/32	1		196	950G19-1	FORGING	MAT'L AMS 5731						
46	1		197	950G19-2	FORGING	MAT'L AMS 5731						
117	1		198	950G31-17	CAP (END)	CRES AISI 347						
127	1		199	-18	CAP (END)	CRES AISI 347						
3	76/200			950G10-19	TUBE, P2	CRES AISI 304		1/16 O.D. - .010 WALL				
3	41		201	950GG7-1	THERMOCOUPLE							
1	12		202	MS9950-505	STUD							
1	12		203	MS51957-105	RING, LOCK							
1	2		204	MS9068-013	RING, SEAL							
3	1		205	950G58-1	TUBE, INLET, 2A	CRES AISI 303		5/8 O.D. - .020 WALL				
G1	1		206	950G15-19	HEADER			MAKE FROM ITEM 192				
G1	1		207	-21	HEADER			MAKE FROM ITEM 192				
G1	1		208	950G06-1	SHELL	MAT'L AMS 5540 Ti-200		.078 SHEET				
G1	7		209	950G59-1	INSERT	MAT'L AMS 5754		.50 DIA BAR				
G1	1		210	85049-0075 -1808	FIN			.005 SHEET				
G1	4		211	85049-0110 -1808	FIN							
G1	1		212	85049-0121 -1807	FIN							
G1	1		213	85049-0131 -1807	FIN							
G1	1		214	85049-0141 -1808	FIN							
G1	1		215	85049-0151 -1818	FIN	MAT'L AMS 5554		.006 SHEET				

ITEM	QTY PER	NEW	OLD	PART NUMBER	DESCRIPTION	MATERIAL	REF.	REMARKS (HEAT TREATING, PLATING PROCESS OF MANUFACTURE, ETC.)	SPEC.	DRAFT.	CHECK.	APPROVAL NUMBERS OF CHECKERS
G9	1	84		950G02-1	SHELL ASSY-COLD							
84	1	85		-3	SHELL, CYLINDER	MAT'L AMS 5643 MAT'L AMS 5544		.312 PLATE				
84	1	86		-5	SHELL, CONE			.312 PLATE				
G9	1	87		950G03-1	SHELL ASSY, HOT							
87	1	88		-3	SHELL, CYLINDER	N-200 AMS 5544 N-200		.375 PLATE				
87	1	89		-5	SHELL, CONE	AMS 5544 N-200		.375 PLATE				
G9	6	90		950G04-1	HEADER, STRUT	MAT'L AMS 5544		.50 PLATE				
G9	1	91		85049-0005 -1004	FIN			.005 SHEET				
G9	1	92		85049-0004 -2516	FIN							
G9	4	93		85049-0100 -1003	FIN							
G9	1	94		85049-0158 -1008	FIN							
G9	4	95		85049-0110 -1004	FIN							
G9	6	96		85049-0150 -0010	FIN							
G9	1	97		85049-0110 -1008	FIN							
G9	3	98		85049-0088 -1004	FIN							
G9	1	99		85049-0110 -2504	FIN							
G9	2	100		85049-0172 -1508	FIN							
G9	1	101		85049-0178 -1508	FIN							
G9	1	102		85049-0078 -1808	FIN							
G9	1	103		85049-0078 -1808	FIN							
G9	2	104		85049-0088 -1808	FIN							
G9	2	105		85049-0084 -1504	FIN							
G9	4	106		85049-0057 -1004	FIN							
G9	10	107		85049-0067 -1008	FIN							
G9	1	108		85049-0078 -1008	FIN							
G9	1	109		85049-0078 -1008	FIN	MAT'L AMS 5544		.005 SHEET				
G1	55	110		950G40-1	INSERT, INSTRUMENT	MAT'L AMS 5754		.250 DIA WIRE				
G1	9	111		950G40-2	INSERT, INSTRUMENT	MAT'L AMS 5754		.250 DIA WIRE				
3	6	112		950G36-1	BOSS, MOUNT, IGNITER	N-200 AMS 5544		1.50-1.50 BAR				
1/64	1	113		950G12-1	PLUG, PROBE ASSY	N-200 AMS 5544		3/4 DIA BAR				
1	6	114		950G13-1	COLLAR	CRES AISI 347		5/16 O.D. - .035 WALL				
3	1	115		950G13-2	COLLAR	CRES AISI 347		5/16 O.D. - .035 WALL				
1	6	116		950G27-1	BODY ASSY, IGNITER							
1	1	117		950G31-1	MANIFOLD ASSY, WATER							
117	1	118		-3	BODY, OUTER			MAKE FROM ITEM 195				
118	1	119		-5	BODY, INNER			MAKE FROM ITEM 194				
119	1	120		-7	FLANGE, INLET	CRES AISI 347		.75 PLATE				
120	1	121		-9	TUBE, INLET	CRES AISI 347		3.00 O.D. - .065 WALL				
121	1	122		-11	TUBE, REDUCER	CRES AISI 347		2.62 O.D. - .065 WALL				
122	1	123		-13	TUBE, TURNING	CRES AISI 347		2.62 O.D. - .065 WALL				
117	1	124		-15	END CAP	CRES AISI 347		.50 PLATE				
127	1	125		-16	END CAP	CRES		.50 PLATE				
117	1	126		-19	SPACER	CRES AISI 347		5/16 DIA BAR				
1	1	127		950G31-2	MANIFOLD ASSY, WATER							
127	1	128		-9	BODY, OUTER			MAKE FROM ITEM 195				
48	9	129		950G25-9	BOSS, INSTRUMENT	CRES AISI 347		3/16 DIA WIRE				
1	2	130		950G38-1	GASKET, PROBE ASSY	VIT. AMS 3217 CLASS 2		.003 SHIM STOCK (ANNEALED)				
1	2	131		950G41-1	PROBE ASSY							
131	1	132		-3	BODY			MAKE FROM ITEM 113				
131	1	133		-5	TUBE	CRES AISI 304		.028 O.D. - .004 WALL				
131	1	134		-7	TUBE							
131	1	135		-9	TUBE							
131	1	136		-11	TUBE							
131	1	137		-15	TUBE							
131	1	138		-15	TUBE	CRES AISI 304 CRES		.028 O.D. - .004 WALL				
1	2	139		950G42-1	NUT, PROBE ASSY	AISI 321		1.00 DIA BAR				
1	1	140		950G45-1	TUBE ASSY, O_2, MID							
140	1	141		-3	TUBE, MANIFOLD	CRES AISI 321		3/8 O.D. - .020 WALL				
140	2	142		-7	TUBE, INLET	CRES AISI 347		V4 O.D. - .020 WALL				
140	1	143		-5	FITTING			MAKE FROM G PIPE PLUG PARKER HANNIFIN				
140	2		144	AN818-4J	NUT							
140	2		145	MS20819-4C	SLEEVE							
1	1	146		950G00-3	MANIFOLD, IN, O_2 IGNITOR			MAKE FROM ITEM 147				
146	1	147		950G47-1	TUBE ASSY, O_2 IN							
147	1	148		-3	TUBE	CRES AISI 321		3/8 O.D. - .020 WALL				
147	2	149		-5	FITTING			MADE FROM G PIPE PLUG PARKER HANNIFIN				
1	1	150		950G00-5	MANIFOLD, LARGE O_2							
150	1	151		950G50-1	TUBE ASSY, LARGE O_2							
15	1	152		-3	TUBE,	CRES AISI 321		3/8 O.D. - .020 WALL				
15	1	153	153	G-4 TRBZ	TUBE END REDUCER			PARKER HANNIFIN				
1	6	154		950G55-1	TUBE ASSY, IGNITOR INLET							
154	1	155		-3	TUBE	CRES AISI 321		V4 O.D. - .020 WALL				
154	1	156		-5	FITTING			MAKE FROM AN821-4J				
1	8	157		950G56-1	TUBE ASSY, EXIT, O_2							
157	1	158		-3	TUBE	CRES AISI 321		V4 O.D. - .020 WALL				
157	1		159	AN818-4C	NUT							
157	1		160	MS20819-4C	SLEEVE							
1	1	161		950G00-13	TUBE	CRES AISI 321		V4 O.D. - .020 WALL				
1	1	162		950G00-7	MANIFOLD, IN, H_2 IGNITOR							
162	1	163		950G51-1	TUBE ASSY, H_2 IN							
163	1	164		-3	TUBE			5/16 O.D. - .028 WALL				
163	1	165		-5	FITTING			MADE FROM G PIPE PLUG PARKER HANNIFIN				
1	1	166		950G00-9	MANIFOLD, MID, H_2 IGNITOR							

ITEM	QTY PER	NEW	OLD	PART NUMBER	DESCRIPTION	MATERIAL	REF.	REMARKS (HEAT TREATING, PLATING PROCESS OF MANUFACTURE, ETC.)	SPEC.	DRAFT.	CHECK.	APPROVAL NUMBERS OF CHECKERS
—	1		1	950G00-1	OUTERBODY ASSY							
—	1		2	950G07-1	GASKET, WATER	SILICONE RUBBER PER EMS 93002						
1	1	3		950G10-1	MANIFOLD ASSY (BRAZED)							
3	1	4		-5	HEADER, AFT			MAKE FROM ITEM 192				
3	1	5		-7	RING, AFT			MAKE FROM ITEM 196				
3	1	6		-9	RING, FWD			MAKE FROM ITEM 196				
3	6	7		-3	PAD, MOUNT, STRUT	MAT'L AMS 5754		3/4 BAR				
3	1	8		-11	MANIFOLD ASSY (3A)			MAKE FROM ITEM 9				
6	1	9		950G35-1	MANIFOLD ASSY, 3A							
9	1	10		-5	TUBE, MANIFOLD	MAT'L P-6007 AMS 5587		1.00 O.D. - .049 WALL				
9	2	11		-5	TUBE, INLET	CRES AISI 321		1.00 O.D. - .049 WALL				
9	1	12		-7	RING			MAKE FROM ITEM 192				
9	1	13		-9	RING			MAKE FROM ITEM 192				
9	2	14		-11	DOUBLER	CRES AISI 321		.050 SHEET				
9	4	15		-13	BOSS, INSTRUMENT	CRES AISI 321		3/16 DIA ROD				
3	1	16		950G10-13	MANIFOLD ASSY (2B)			MAKE FROM ITEM 17				
16	1	17		950G34-1	MANIFOLD ASSY, 2B							
17	1	18		-3	TUBE, MANIFOLD	MAT'L P-6007 AMS 5587		1.06 O.D. - .049 WALL				
17	2	19		-5	TUBE, INLET	CRES AISI 321		1.00 O.D. - .049 WALL				
17	2	20		-7	RING			MAKE FROM ITEM 192				
17	2	21		-9	DOUBLER	CRES AISI 321		.050 SHEET				
17	4	22		-11	BOSS, INSTRUMENT	CRES AISI 347		3/16 DIA ROD				
3	1	23		950G10-15	MANIFOLD ASSY (2A)			MAKE FROM ITEM 24				
23	1	24		950G28-1	MANIFOLD ASSY, 2A							
24	1	25		-9	TUBE, MANIFOLD	MAT'L P-6007 AMS 5587		.81 O.D. - .049 WALL				
24	2	26		-7	DOUBLER	CRES AISI 321		.050 SHEET				
24	2	27		-9	RING			MAKE FROM ITEM 192				
24	4	28		-5	BOSS, INSTRUMENT	CRES AISI 347		3/16 DIA ROD				
24	1	29		950G48-1	TUBE, INLET, 2A, LEFT	CRES AISI 347		G3 O.D. - .020 WALL				
24	1	30		950G49-1	TUBE, INLET, 2A, RIGHT	CRES AISI 347		G3 O.D. - .020 WALL				
3	1	31		950G10-17	MANIFOLD ASSY (4)			MAKE FROM ITEM 32				
31	1	32		950G28-1	MANIFOLD ASSY, 4							
32	1	33		-5	TUBE, MANIFOLD	MAT'L P-6007 AMS 5587		1.13 O.D. - .049 WALL				
32	2	34		-7	CAP, TUBE	CRES AMS 5536		.125 SHEET				
32	2	35		-5	RING			MAKE FROM ITEM 192				
32	2	36		-9	CAP, END	CRES AISI 347		.125 SHEET				
32	1	37		-11	DOUBLER	CRES AISI 321		.050 SHEET				
32	4	38		-13	BOSS, INSTRUMENT	CRES AISI 347		3/16 DIA WIRE				
32	1	39		950G08-1	TUBE ASSY, INLET, 4							
39	1	40		-9	TUBE	CRES AISI 321		1.00 O.D. - .035 WALL				
39	1	41		-5	FLANGE	AISI 321		.25 PLATE				
3	1	42		950G10-23	MANIFOLD ASSY (1B)			MAKE FROM ITEM 43				
42	1	43		950G11-1	MANIFOLD ASSY, 1B							
43	94	44		-3	TUBE, CROSSOVER	MAT'L P-6007 AMS 5587		3/16 O.D. - .016 WALL				
43	1	45		950G09-1	RING ASSY, L.E.							
45	1	46		-3	RING			MAKE FROM ITEM 193				
45	1	47		-5	RING			MAKE FROM ITEM 197				
43	1	48		950G25-1	RING ASSY, MANIFOLD 1B							
48	1	49		-3	TUBE, MANIFOLD	MAT'L P-6007 AMS 5587		1.00 O.D. - .049 WALL				
48	1	50		-5	RING			MAKE FROM ITEM 192				
48	1	51		-7	DOUBLER	CRES AISI 321		.050 SHEET				
48	1	52		950G26-1	TUBE ASSY							
52	1	53		-5	TRANSITION	CRES AISI 321		.032 SHEET				
52	1	54		-7	TUBE	CRES AISI 321		1.00 O.D. - .035 WALL				
52	2	55		-9	SHEET	CRES AISI 321		.063 SHEET				
52	1	57		-3	FLANGE	CRES AISI 321		.25 PLATE				
3	1	58		950G10-21	MANIFOLD, WATER			MAKE FROM ITEM 59				
58	1	59		950G30-1	MANIFOLD, WATER			MAKE FROM ITEM 191				
3	1	60		950G15-1	INJECTOR ASSY							
G0	1	61		-3	BRAZE ASSY							
G1	2	62		-5	INSERT, PROBE	MAT'L P-6007 AMS 5587		1.00 DIA BAR				
G1	6	63		-7	INSERT, IGNITER	MAT'L P-6007 AMS 5587		.688 O.D. - .049 WALL				
G1	120	64		-9	INJECTOR, 3A	MAT'L P-6007 AMS 5587		3/16 O.D. - .049 WALL				
G1	22	65		-11	INJECTOR, 2B	MAT'L P-6007 AMS 5587		5/16 O.D. - .049 WALL				
G1	22	66		-13	INJECTOR, 2A	MAT'L P-6007 AMS 5587		1/4 O.D. - .049 WALL				
G1	28	67		-15	INJECTOR, 4	MAT'L P-6007 AMS 5587		V4 O.D. - .049 WALL				
G1	96	68		-17	INJECTOR, 1B	MAT'L P-6007 AMS 5587		3/16 O.D. - .049 WALL				
G1	1	69		950G01-1	SHELL ASSY							
69	1	70										
69	2	71										
69	2	72										
69	2	73										
69	2	74										
69	1	75		-17	HEADER			MAKE FROM ITEM 192				
69	1	76		-19	HEADER			MAKE FROM ITEM 192				
69	1	77										
69	2	78										
69	1	79										
69	1	80		85049-0006 -1004	FIN	MAT'L AMS 5554		.006 SHEET				
69	2	81		85049-0104 -1004	FIN							
69	3	82		85049-0100 -1003	FIN							
69	2	83		85049-0100 -1004	FIN	MAT'L AMS 5554		.006 SHEET				

⚠ MACHINE THIS SURFACE TO WITHIN ±.003 OF COMPUTER READOUT (AERODYNAMIC CONTOUR).
10. ALL BRAZE JOINTS TO BE MACHINED AT ASSY TO PROVIDE .001-.003 BRAZING GAP.
9. ALL INJECTOR HOLES TO BE EQUALLY SPACED ∢ INDEXED FROM TOP ℄ EXCEPT AS SHOWN.
⚠ DYE PENETRANT INSPECT PER MIL-I-6866 ∢ RADIOGRAPHIC INSPECT PER MIL-STD-453.
⚠ DYE PENETRANT INSPECT PER MIL-I-6866 ∢ RADIOGRAPHIC INSPECT PER MIL-R-11468.

⚠ FURNACE BRAZE PER AIRESEARCH SPEC WBS-27 (EXCEPT OMIT PEEL TEST SAMPLES) USING ASTM 260 CLASS BA3-BA BRAZING ALLOY.
⚠ FURNACE BRAZE PER AIRESEARCH SPEC WBS-27 (EXCEPT OMIT PEEL TEST SAMPLES) USING EMS 94087 (PALNIRO 7) BRAZING ALLOY.
⚠ FURNACE BRAZE PER AIRESEARCH SPEC WBS 27 (EXCEPT OMIT PEEL TEST SAMPLES) USING PALNIRO "RC" GRADE BRAZING ALLOY.
⚠ FURNACE BRAZE PER AIRESEARCH SPEC WBS 27 (EXCEPT OMIT PEEL TEST SAMPLES) USING EMS 94087 (PALNIRO 2) BRAZING ALLOY.
⚠ WELD PER AIRESEARCH SPEC WBS-18.
⚠ WELD PER AIRESEARCH SPEC WBS-35
NOTE: UNLESS OTHERWISE SPECIFIED

AIRESEARCH MANUFACTURING COMPANY
A DIVISION OF THE GARRETT CORPORATION
LAYOUT

SIGNATURES	DATES	DATE STARTED	WITHDRAWN BY
GALLAGHER	1-30-73		
	1-22-73	DATE COMPLETED	
	1-22-73		
	2-2-73	DRAWING NO.	
	6-5-73	950052-33-0100	

OUTERBODY
BOILERPLATE H.R.E.

SIZE 70210 | CODE IDENT NO. | DRAWING NO. L950991
SCALE | WT | SHEET 1 OF 3

UNCLASSIFIED

UNCLASSIFIED

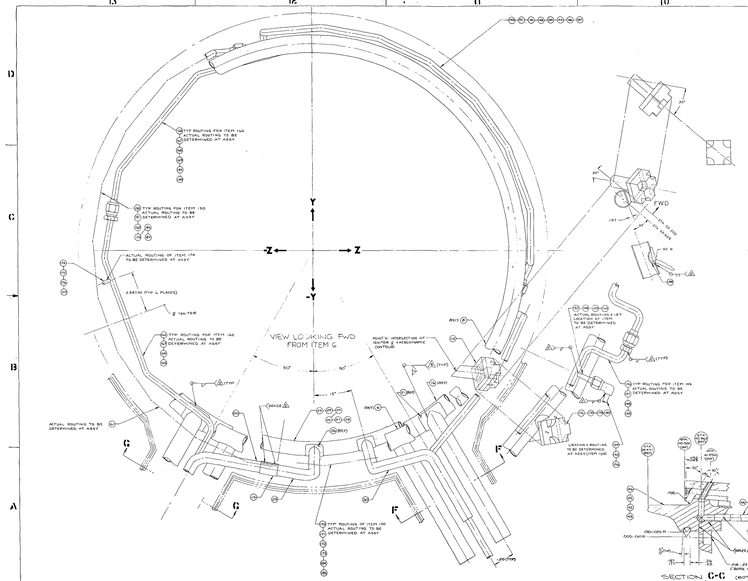

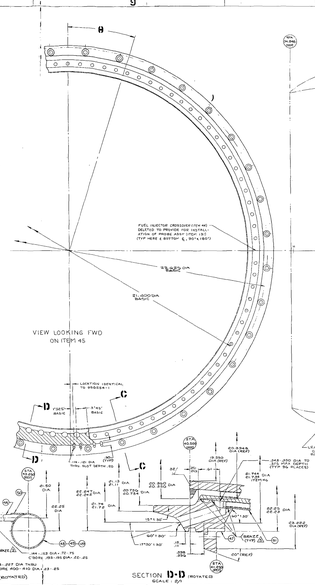

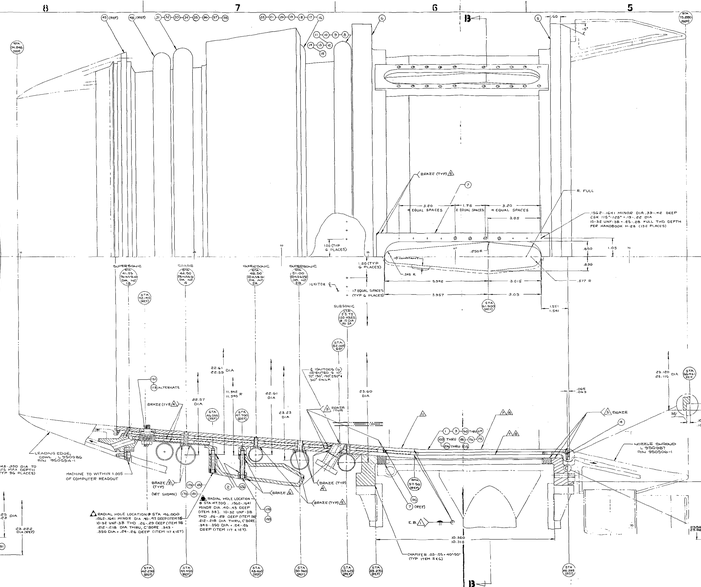
B
B
SUPERSONIC
FLOW
SUBSONIC
FLOW
SUPERSONIC
FLOW
SUBSONIC
FLOW
BASIC
BASIC
BASIC

UNCLASSIFIED

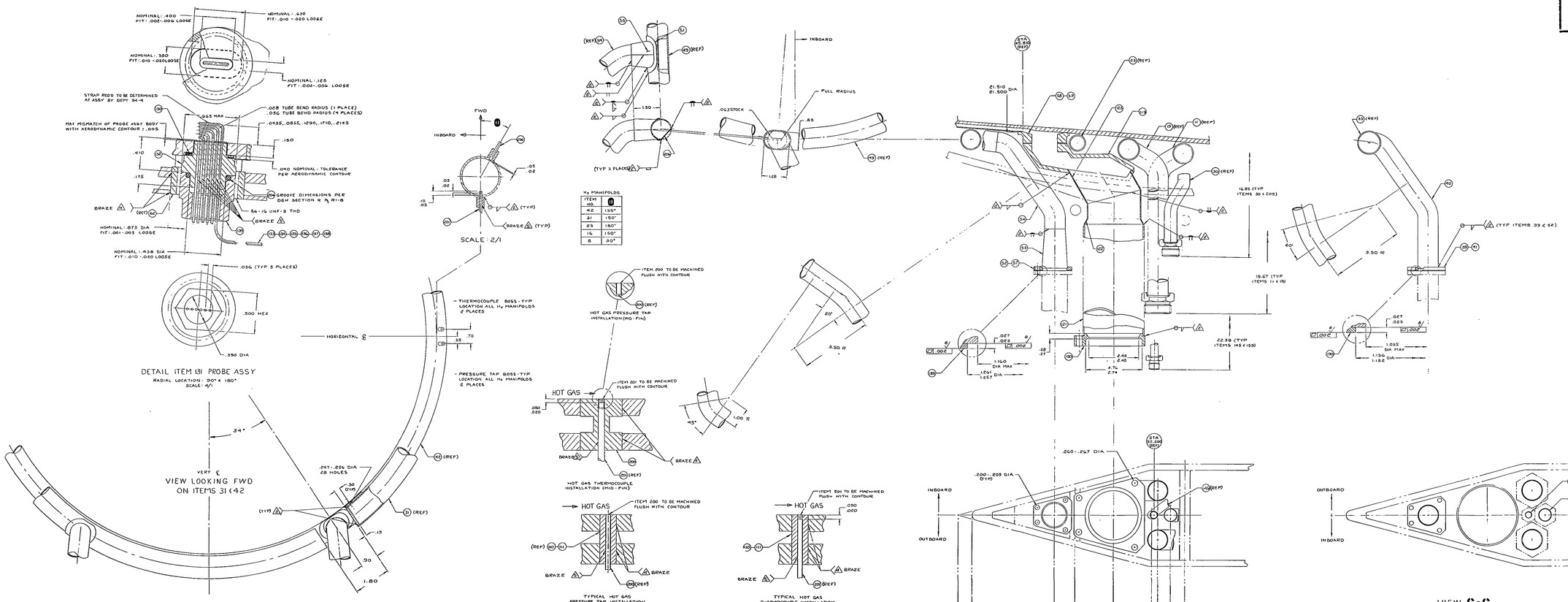

UNCLASSIFIED

MODIFIERS	DATE	APPD.	ORIGINATOR
MECHANICS	10-1-63		BY
Stress Analysis	10-15-63		
Thermodynamics	10-15-63		
Aerodynamics	10-15-63		
Weights	10-15-63		CHECKED
Reliability	10-15-63		BY
Quality Control	10-15-63		
Manufacturing	10-15-63		
Engineering	10-15-63		
		1-5000E-33-0100	

AIRESEARCH MANUFACTURING COMPANY
A DIVISION OF THE GARRETT CORPORATION
LAYOUT

OUTERBODY
BOILERPLATE H.R.E.

SIZE D | AIRESEARCH NO. 70210 | L950991

SCALE | WT | SHEET 3 OF 3

UNCLASSIFIED

UNCLASSIFIED

REVISIONS			
LTR	DESCRIPTION	DATE	APPROVED

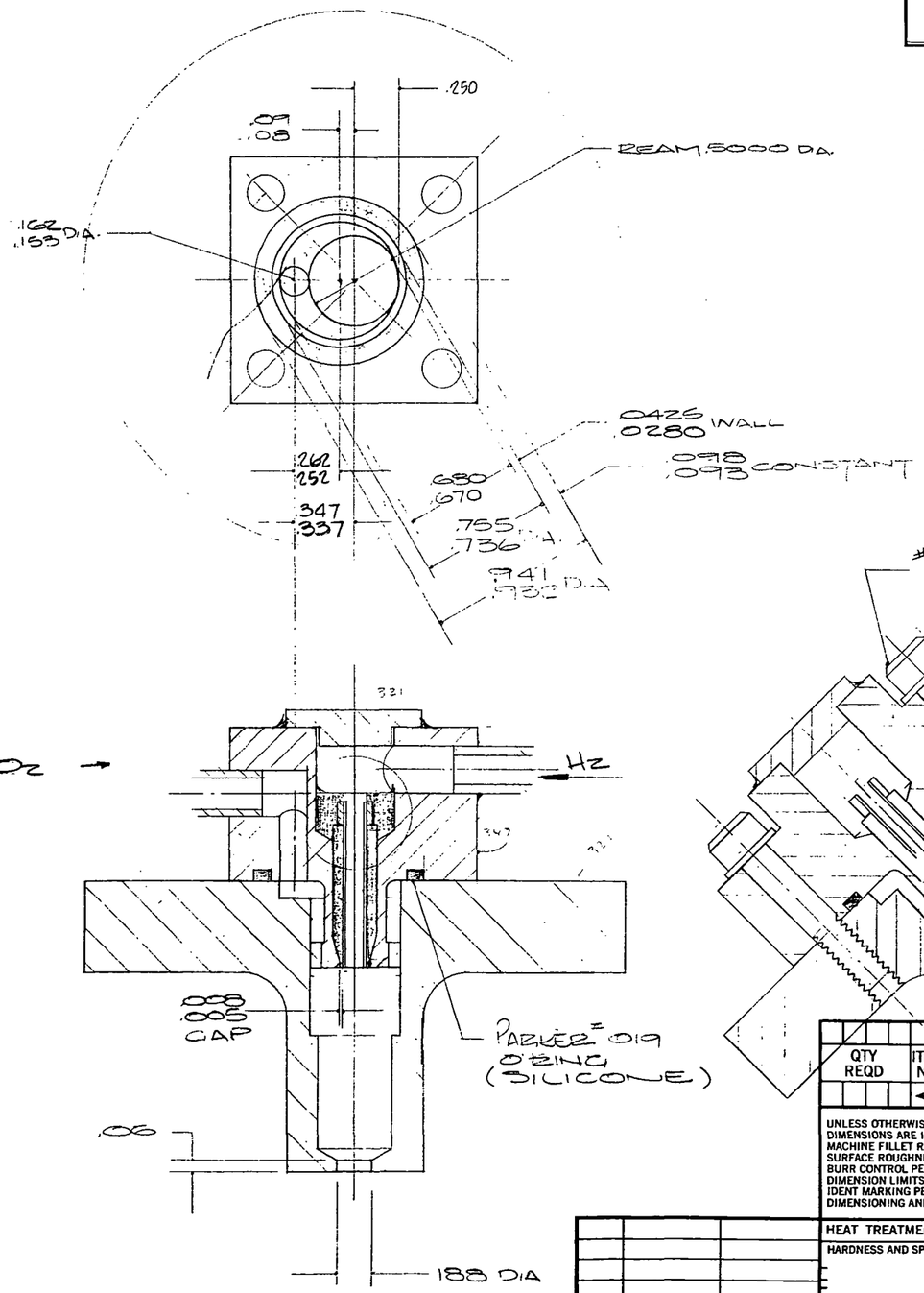

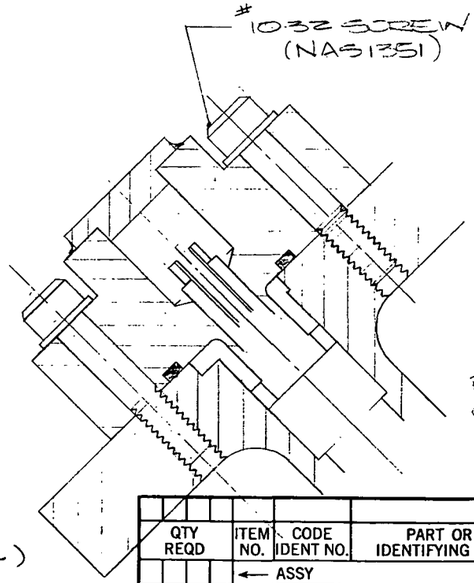

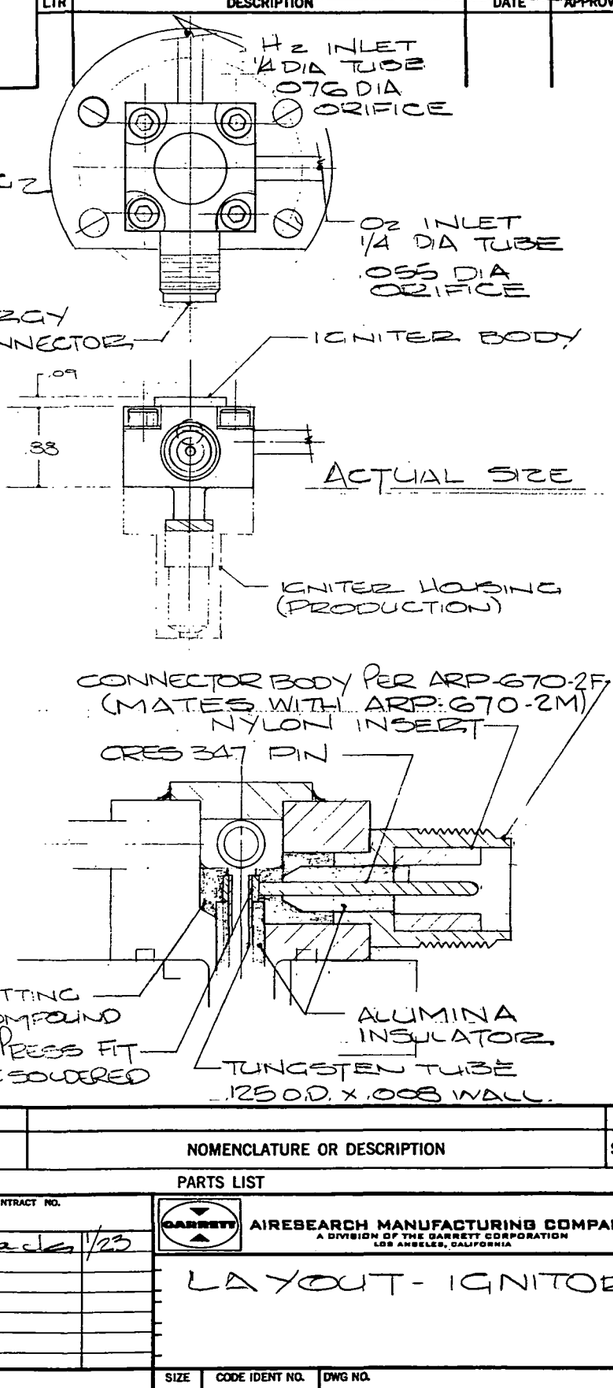

QTY REQD	ITEM NO.	CODE IDENT NO.	PART OR IDENTIFYING NO.	NOMENCLATURE OR DESCRIPTION	SYM
	← ASSY			PARTS LIST	

UNLESS OTHERWISE SPECIFIED:
DIMENSIONS ARE IN INCHES.
MACHINE FILLET RADII .015 — .030
SURFACE ROUGHNESS PER USAS B46.1-62
BURR CONTROL PER SC653
DIMENSION LIMITS HELD AFTER PLATING
IDENT MARKING PER MC16
DIMENSIONING AND TOL PER USAS Y14.5-66

CONTRACT NO.

DFS	S Kopacka	1/23
CHK		
VALUE ENGR		
MATL		
STRESS		
APPD		
APPD		
AIRESEARCH APPD		
OTHER ACTIVITY APPD		

AIRESEARCH MANUFACTURING COMPANY
A DIVISION OF THE GARRETT CORPORATION
LOS ANGELES, CALIFORNIA

LAYOUT - IGNITOR

SIZE	CODE IDENT NO.	DWG NO.
C	70210	PA 106753

SCALE 2/1 SHEET OF

REQD	NEXT ASSY	USED ON
APPLICATION		

HEAT TREATMENT	PROCESS
HARDNESS AND SPEC	NAME AND SPEC

REV LETTER DWG NO.

UNCLASSIFIED

TABLE OF CONTOUR COORDINATES

A	27.140	26.196	25.007	23.809	22.670	21.650	19.625	18.734	17.600	16.596	15.845	15.140	12.740	11.420	7.790
B	3.237	3.411	3.633	3.885	4.122	4.338	4.782	4.985	5.256	5.518	5.726	5.926	6.660	7.190	8.607
LAYOUT STATION (REF)	18.360	19.304	20.443	21.691	22.830	23.850	25.875	26.766	27.900	28.904	29.655	30.360	32.760	34.080	37.710

7.430	6.962	6.674	6.368	5.720	5.000	3.500	2.100	1.500	.500	-.500	-1.500	-2.100	-2.900	-10.260
8.735	8.874	8.942	9.000	9.096	9.180	9.318	9.415	9.452	9.518	9.578	9.624	9.650	9.670	9.670
38.070	38.538	38.826	39.132	39.780	40.500	42.000	43.400	44.000	45.000	46.000	47.000	47.600	48.900	55.760

TABLE OF INSTRUMENTATION TYPE AND LOCATION

B	44.905	31.100	21.500	14.900	10.500	10.000	9.800	9.500	9.000	8.500	8.000	7.500	7.500	7.000	6.500
CIRCUMFERENTIAL LOCATION	℄	0° 90° 180° 270°	0°	0°	0° 90° 180° 270°	0°	5°	0°	0° 90° 180° 270°	0°	0°	0° 90° 180° 270°	5°	0°	0° 90° 180° 270°
LAYOUT STATION (REF)	.595	14.400	24.000	30.600	35.000	35.500	35.700	36.000	36.500	37.000	37.500	38.000	38.000	38.500	39.000
TYPE	7	7	9	7	7	7	9	7	8	8	7	7	9	7	7

6.000	5.500	5.500	4.000	3.500	3.500	3.500	3.000	1.800		.500	0.500	-.700	-1.300	-2.000	INJECTOR MANIFOLDS TEMP.	INJECTOR MANIFOLDS PRESS.
0°	0° 90° 180° 270°	5°	0°	180° 270°	180° 270°	0°	0°	0° 90° 180° 270°		5°	0°	5°	0° 90° 180° 270°	0°	180° 330°	185° 335°
39.500	40.000	40.000	41.500	42.000	42.000	42.000	42.500	43.700		45.000	45.000	46.200	46.800	47.500	1A 21C (TOTAL 4)	1A 21C (TOTAL 4)
7	8	11	7	TOTAL PRESSURE RAKE	STAT PRESS ON T.P. RAKE	9	7	8		10	8	10	8	8	10	8

LTR	ZONE	DESCRIPTION	DATE	APPROVED
K	5C	INC. A.R.N. DTD 4-17-69 (WELD ITEM 35)	5-23-9	
L	2C 3C	INC. A.R.N. DTD 4-28-69 (JOINT ITEM 2/4)	5-23-9	
M	2B 1B 1A 1A 3A 9A 12A 9A 12A	1) ADDED ITEMS 63 THRU 75 2) DELETED ITEMS 32,33,42,44,45,57. 3) QTY ITEM 25 IS 2 (WAS 1) 4) MATL ITEM 1 ZrCu (WAS OFHC) 5) ADDED NOTE 29. MATL. SPEC. ITEM 1. 12) DELETED INSTRUMENTATION AT STAS. 44.3, 44.5, 45.5, 46.0. 13) ADDED INSTR AT STA 45.1 AND 46.1 AND 1C MANIFOLD	5-23-9	R
N	1A 2B 1A 5A 5A 8D 12C	1) DELETED AND ERASED ITEMS 25,32,33,42,45,66 2) ADDED ITEMS 76-80 3) ITEM 8 PART NO 950667-1 (WAS PA 93506) 4) ADDED 2 HOLES TO ITEM 16 5) ADDED CUT-OUT IN ITEM 19. FOR ITEM 81 6) INSTR. DIMS 49-51 (WAS 41-39). 69-71 (WAS 49-51) 7) INSTR TABLE STA. 45.0 (WAS 45.1) 46.2 (WAS 46.0). DELETED STA 44.3 ENTRY 10) SEE DRAWING REVISION NOTICE		R

REVISIONS

LTR	ZONE	DESCRIPTION	DATE	APPROVED
A		INC ARN DTD 8-13-68 (SEE SH 2)		R
B	1, 6A, 2, 8B, 9A, 8A, 8, 2, 5,1	1). ADDED ITEM 56 TO LIST OF MATERIALS DELETED ITEM 30. 2). ADDED VIEW SHOWING ITEM 56 & SLOT 3). ADDED: BEFORE FINAL MACHINING TO G/N 20. 4). ADDED 18.91-18.93 TO SECT D-D 5). 4.66-4.70 WAS 4.47-4.53 ITEM 24 REVISED TO INCLUDE RING EXPANSION JOINT, ITEM 49 NOW CALLS OUT REVISED MANIFOLD ELBOW SECT. ADDED 3 INSTRUMENTATION TUBES AT STAS 40, 42.5, 49.3 WATER PASSAGE HEIGHT .05-.08 WAS .05-.07 6). ADDED ITEM 57 AND CUT-OUT IN ITEM 42. 7). BAG 8A BRAZE MATERIAL WAS BAG-5 QQ-S-561 (NOTE 3) 8). ADDED ITEMS 58, 59, 60.		R
C		INC ARN DTD 12-13-68 (ADDED G/N 24)		
D	2C, 8A, 9D, 8/11, 2B 2B 8/11	1) DIMENSION -1.300 WAS -1.800 AND -2.000 WAS -2.500 (TABLE OF INST) 2) "PASSAGE HEIGHT .04-.06 ---- ETC. WAS .05-.08 PASSAGE BETWEEN STA 40.7 AND 48.8. 3) DELETED REF ON DIM. 3.96-3.98. 4) DELETED ITEM 3 FROM H/O AND B/M AND MODIFIED ITEM 2 5) ITEM 25 1 REQD WAS 2 REQD 45 1 REQD WAS 2 REQD 24 ADDED "FORGING" IN MATL COLUMN 6) ADDED NOTE 25 7) ITEM 18 QTY 37 (WAS 24)		
E	9A 10C	INC. ARN. DTD 2-7-69 (WELD SALVAGE)		
F	1B, 1C, 1C, 2C, 2B, 2B, 1B, 2A, 12C, 8D, 3B, 6B, 1A, 1C	1 ITEM 41. QTY 15 (WAS) 11 AND MAKE FROM .156 O.D. (WAS) .125 O.D. 2 ITEM 58. AN 960-C4L (WAS) 950512-127 3 ITEM 59. MS 35649-244 (WAS) 950512-129 4 INSTR. TABLE. INJECTOR MANIFOLD TEMP ADDED 180° & INJECTOR MANIFOLD PRESS ADDED 185° 5 ITEM 47 950512-133 (WAS) 950512-113 6 DELETED ITEM 46. 950512-109-CLAMP PLATE, IGNITER, .200 THICK CRES AISI 321 7 ITEM 8. WAS 950512-19 8 BRAZE WAS PALNIRO 7. 9 BRAZE WAS 10 BRAZE WAS 11 CHANGE 3 WELDS TO . WAS TYP 6 PLACES. 12 2.68 2.66 DIM WAS 2.71 2.69 13 ADD NOTE "M/C PILOT OPP. WELD ENTRY" 14 ADDED ITEMS 61 & 62 TO PARTS LIST		R
G	9	INC ARN DTD 4/8/69 (SALVAGE ITEM 17)		
H	2	INC ARN DTD 4/8/69 (SALVAGE ITEM 17)		
J	2B	ADDED NOTE 28 & CALLOUT (CONT)		R

PARTS LIST

QTY REQD	ITEM NO.	CODE IDENT NO.	PART OR IDENTIFYING NO.	NOMENCLATURE OR DESCRIPTION	SYM	ZONE
1	80		-179	RING, CONE STIFFENING CRES AISI 321		
4	79		-177	BOSS, MOUNTING .50 DIA ROD CRES AISI 321		
1	78		-175	BLOCK 1.00 x .50 BAR CRES AISI 321		
6	77		-173	NOZZLE, IGNITER NI 200 .375 □ STOCK		
2	76		-169	EXPANSION RING .020 THICK CRES AISI 321		
1	75		-167	MOUNTING RING CRES AISI 321		
1	74		-165	CONE RING CRES AISI 321		
1	73		-163	OUTER SKIN NI 200 FORGING		
1	72		-159	FLANGE 2.2500 x .062 WALL CRES AISI 321		
1	71		-157	TRANSITION HALF .050 SHEET CRES AISI 321		
1	70		-155	TRANSITION HALF .050 SHEET CRES AISI 321		
1	69		-154	ELBOW HALF .050 SHEET CRES AISI 321		
1	68		-153	ELBOW HALF .050 SHEET CRES AISI 321		
1	67		-149	MANIFOLD 1.0 OD x .050 WALL TUBE CRES AISI 321		
1	66		-147	STIFFENER INCO 600 FORG.		
1	65		-145	INJECTOR RING NI 200 FORG.		
1	63		-139	INNER SHELL INCO 600 FORG.		

LIST OF MATERIAL

QTY REQD	ITEM NO.	PART NO.	SYM	DESCRIPTION	CODE IDENT	MATERIAL AND SPECIFICATION	ZONE
4	62	-137		BOSS, ELBOW MOUNT		.500 .499 DIA STOCK CRES AISI 321	19
1	61	-135		BOSS, ELBOW SUPPORT		.51 .49 STOCK PLATE CRES AISI 321	19
AR	60	-131		TUBE, INSTRUMENTATION		.028 O.D. x .004 WALL	
4	59	MS35649-244		NUT, PLAIN			7
4	58	AN960-C4L		WASHER, PLAIN			7
1	57	-125		WALL SECTION, OUTER		MAKE IT W/ FORGING NI 200	2
2	56	-123		PLATE, MOUNTING		AMS 3617 (NYLON)	7
1	55	-119		BRACKET WATER TUBE		.100 THICK CRES AISI 321	9
1	54	950524-5		FLANGE, O'RING		CRES AISI 321	8
1	53	950513-1		SKIRT ASSEMBLY			8
1	52	950514-1		TIP, COOLING TUBE MANIFOLD		CRES AISI 347	12
4	51	-117		TUBE		.250 O.D. x .020 WALL CRES AISI 321	11
1	50	950526-1		TUBE ASSEMBLY			12
1	49	950524-1		TUBE ASSEMBLY			12
1	48	-115		FLANGE, INJECTOR		2.25 O.D. x .82 WALL CRES AISI 321	13
1	43	-103		RING, CONE STIFFENING		.250 THICK CRES AISI 321	24
13	41	-97		INSTRUMENTATION BOSS		.1560 D CRES AISI 347	8
1	40	-96		REINFORCEMENT, ELBOW		.188 THICK CRES AISI 321	24
1	39	-95		REINFORCEMENT, ELBOW		.188 THICK CRES AISI 321	24
1	38	-94		SUPPORT MANIFOLD ELBOW		.188 THICK CRES AISI 321	24
1	37	-93		SUPPORT MANIFOLD ELBOW		.188 THICK CRES AISI 321	24
1	36	-89		ELBOW, MANIFOLD		2.750 OD x .100 WALL CRES AISI 321	8
1	35	-87		RING, MANIFOLD		3.000 OD x .100 WALL CRES AISI 321	8
1	34	-85		INNER WALL, MANIFOLD		MAKE FROM 950517-43 INCO 600	8
1	31	-77		WALL SECTION, OUTER		MAKE FROM FORGING NI 200	8
1	29	-73		ELBOW, INJECTOR MANIFOLD		1.250 OD x .050 WALL CRES AISI 321	18
1	28	-69		TUBE SECTION, ELBOW		.050 WALL CRES AISI 321	19
1	27	-61		MANIFOLD, INJECTOR		1.000 OD .050 WALL CRES AISI 321	8
1	26	-65		RING, INJECTOR		MAKE FROM 950517-15 NI 200	9
1	24	-59		WALL SECTION, INNER		FORGING CRES AISI 321	9
1	23	-57		WALL SECTION, OUTER		MAKE FROM 950517-37 NI 200	9
1	22	-55		RING, CONE STIFFENING		.250 THICK CRES AISI 321	19
1	21	-53		RING, CONE STIFFENING		3.125 OD .313 WALL CRES AISI 321	9
1	20	-49		FLANGE, MOUNTING CONE		MAKE FROM 950516-7 CRES AISI 321	8
1	19	-47		CONE, MOUNTING		.200 THICK CRES AISI 321	9
37	18	-45		BOSS, INSTRUMENTATION		.375 OD x .030 WALL CRES AISI 321	26
1	17	-43		CONE SECTION, INNER		.125 THICK CRES AISI 321	9
1	16	-39		RING, CONE SUPPORT		MAKE FROM 950516-35 CRES AISI 321	10
1	15	-37		CONE SECTION, INNER		.125 THICK CRES AISI 321	10
1	14	-35		RING, CONE SUPPORT		MAKE FROM 950516-37 CRES AISI 321	10
1	13	-33		CONE SECTION, INNER		.125 THICK CRES AISI 321	10
1	12	-29		RING, CONE SUPPORT		MAKE FROM 950516-39 CRES AISI 321	10
1	11	-27		CONE SECTION, INNER		.125 THICK CRES AISI 321	11
6	10	-25		GUSSET PLATE		.080 THICK CRES AISI 321	10
1	9	-23		RING, CONE JUNCTION		MAKE FROM 950517-3 NI 200	9
8	8	950667-1		THERMOCOUPLE		.062 DIA CHROMEL ALUMEL	10
AR	7	-17		TUBE, STATIC PRESSURE		.062 OD x .010 WALL CRES AISI 347	11
1	6	-15		CONE SECTION, OUTER		MAKE FROM 950517-35 NI 200	10
1	5	-13		CONE SECTION, OUTER		MAKE FROM 950517-33 NI 200	10
1	4	-9		CONE SECTION, OUTER		MAKE FROM 950517-31 NI 200	11
1	2	-5		CONE, SPIKE TIP		FORGING NI 200	12
1	1	-3		TIP, SPIKE		1 DIA BAR x 2" LONG. Zr Cu	12

29. "AMZIRC" FROM AMERICAN METAL CLIMAX INC. HEAT TREATED TO FOLLOWING MIN. PROPERTIES:- UTS - 45,000 PSI; YIELD STRENGTH (.2% OFFSET) = 38,000 PSI; ELONGATION = 12%
28. BRAZE PER WBS 27 USING PALNIRO 7
27. TO FACILITATE MANUFACTURE, ITEM 17 MAY BE MADE FROM MORE THAN ONE PIECE. ANY ADDITIONAL WELD JOINTS MUST CONFORM TO WELD NOTE 4
26 TOOLING NEEDED TO RESTRICT RADIAL GROWTH TO .060 ON DIAMETER AT STATIONS 38.5 AND 43.5 DURING PROOF PRESSURE TEST.
25. THESE INSTRUMENTATION BOSSES TO BE LOCATED CIRCUMFERENTIALLY AT 0°, 5°, 10°, 90°, 95°, 175°, 180°, 185°, 270°, 275°, & 355° FROM DATUM 0°
24 ALL OUTER SHELL THERMOCOUPLE JUNCTIONS TO BE LOCATED .145-.155 FROM INNER SURFACE.
23. BOND ITEMS 56, 58, 59 TO INNER SHELL USING POLYURETHANE BOND U-136 APPLIED PER SPEC RS 149
22 STATIC PRESSURE TEST ASSEMBLY TO 300 P.S.I.A. BEFORE FINAL MACHINING
21. CHEMICAL COMPOSITION OF NI 200 PER ASTM B 160 (FORGINGS), B162 (SHEET)
20 ALL TABULATED DIMENSIONS ARE BASIC
19 ALL MACHINED SURFACES 125
18 ALL THREADS TO BE PER HANDBOOK H28
17 ALL FILLET RADII .19 .11
16 FINAL PART TO BE STAMPED OR TAGGED: NASA RAMJET R&D
15. THIS INSTRUMENTATION BOSS TO BE LOCATED CIRCUMFERENTIALLY AT 5° FROM DATUM 0°
14. THESE INSTRUMENTATION BOSSES TO BE LOCATED CIRCUMFERENTIALLY AT 0° 5° 10° 15° 90° 95° 180° 185° 270° 275° 350° 355° FROM DATUM 0°
13. THIS INSTRUMENTATION BOSS TO BE LOCATED CIRCUMFERENTIALLY ON DATUM 0°
12. THESE INSTRUMENTATION BOSSES TO BE LOCATED CIRCUMFERENTIALLY AT 0°, 5° FROM DATUM 0°
11. THESE INSTRUMENTATION BOSSES TO BE LOCATED CIRCUMFERENTIALLY AT 0°, 90°, 180°, 270°. FROM DATUM 0°
10. THERMOCOUPLE BRAZED THRU
9. THERMOCOUPLE THRU CLEARANCE HOLE
8. PRESSURE TUBE BRAZED OR WELDED THRU
7. PRESSURE TUBE THRU CLEARANCE HOLE
6. INSTRUMENTATION TUBES TO BE INSTALLED LONG ENOUGH TO REACH 4.50 AFT OF PLANE 'A'. ALLOWANCE MUST THEN BE MADE FOR 4.25 EXTENSION DURING SPIKE TRAVEL.
5. WELD PER WBS 18
4. ELECTRON BEAM (E.B.) PER WBS 35
3. BRAZE PER WBS 27 USING BAg8A
2. BRAZE PER WBS 27 USING NICORO 80 (EMS 94839)
1. BRAZE PER WBS 27 USING PALNIRO NO. 1 (EMS 94827)

NOTES: UNLESS OTHERWISE SPECIFIED

NEXT ASSY	USED ON
950502-1	960500-1-1

APPLICATION

UNLESS OTHERWISE SPECIFIED: DIMENSIONS ARE IN INCHES. MACHINED FILLET RADII .015 - .030. SURFACE ROUGHNESS PER MIL-STD-10. DIMENSION LIMITS HELD AFTER PLATING. BURR CONTROL PER SPEC SC-653

SIGNATURES / DATES: 6-26-68, 7-12-68, 7-15-68, 7-15-68, 7-16-68, 7-12-68, 7-17-68

AIRESEARCH MANUFACTURING COMPANY

INLET SPIKE ASSEMBLY - NON REPAIRABLE

CODE IDENT NO. 70210 DWG NO. 950512 SCALE 1/1 & NOTED SHEET 1 OF 2

DWG. NO. 950512 SHEET 1

UNCLASSIFIED
UNCLASSIFIED

UNCLASSIFIED

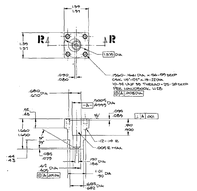

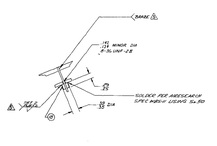

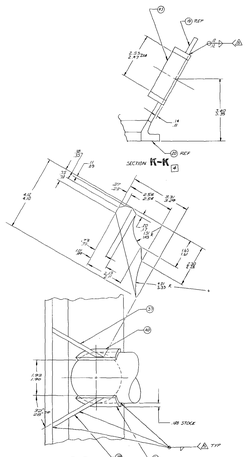

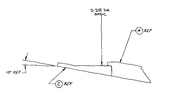

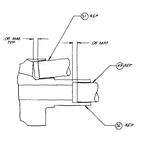

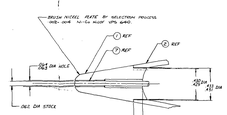

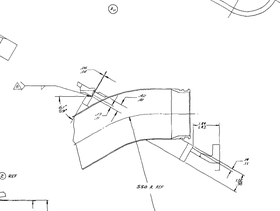

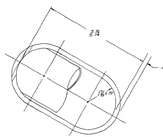

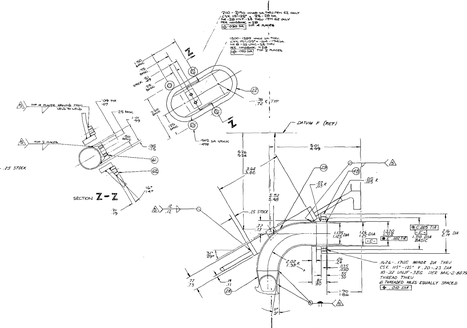

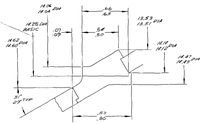

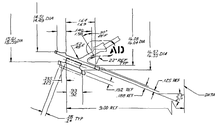

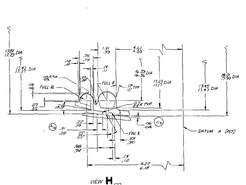

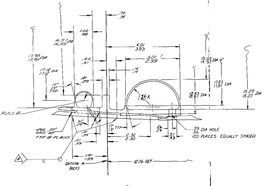

REVISIONS			
ZONE	DESCRIPTION	DATE	APPROVED
PWR A	PER ECN 350512 DATED 10-20-2021	10-20-2021	

CONFIDENTIAL
"This material contains information affecting the National Defense of the United States within the meaning of the Espionage Laws, Title 18, U. S. C. Sec. 793 and 794, the transmission or revelation of which in any manner to an unauthorized person is prohibited by law"

CONFIDENTIAL
"This material contains information affecting the National Defense of the United States within the meaning of the Espionage Laws, Title 18, U. S. C. Sec. 793 and 794, the transmission or revelation of which in any manner to an unauthorized person is prohibited by law"